Environment International 135 (2020) 105345

Contents lists available at ScienceDirect

Environment International

journal homepage: www.elsevier.com/locate/envint

Source apportionment of particle number size distribution in urban background and traffic stations in four European cities

Ioar Rivas[a,*], David C.S. Beddows[b], Fulvio Amato[c], David C. Green[a], Leena Järvi[d,e], Christoph Hueglin[f], Cristina Reche[c], Hilkka Timonen[g], Gary W. Fuller[a], Jarkko V. Niemi[h], Noemí Pérez[c], Minna Aurela[g], Philip K. Hopke[i], Andrés Alastuey[c], Markku Kulmala[d], Roy M. Harrison[b,j], Xavier Querol[c], Frank J. Kelly[a]

[a] MRC-PHE Centre for Environment and Health, Environmental Research Group, King's College London, 150 Stamford Street, London SE1 9NH, UK
[b] Division of Environmental Health & Risk Management, School of Geography, Earth & Environmental Sciences, University of Birmingham, Edgbaston, Birmingham B15 2TT, UK
[c] Institute of Environmental Assessment and Water Research, IDAEA-CSIC, C/Jordi Girona 18–26, 08034 Barcelona, Spain
[d] Institute of Atmospheric and Earth System Sciences/Physics, Faculty of Science, University of Helsinki, P.O. Box 64, FI-00014, Finland
[e] Helsinki Institute of Sustainability Science, Faculty of Science, University of Helsinki, FI-00014, Finland
[f] Laboratory for Air Pollution and Environmental Technology, Swiss Federal Laboratories for Materials Science and Technology (EMPA), Dübendorf, Switzerland
[g] Atmospheric Composition Research, Finnish Meteorological Institute, P.O. Box 503, FI-00101 Helsinki, Finland
[h] Helsinki Region Environmental Services Authority (HSY), Air Protection Unit, P.O. Box 100, FI-00066 Helsinki, Finland
[i] Center for Air Resources Engineering and Science, Clarkson University, Potsdam, NY 13699, USA
[j] Department of Environmental Sciences/Centre of Excellence in Environmental Studies, King Abdulaziz University, PO Box 80203, Jeddah 21589, Saudi Arabia

ARTICLE INFO

Handling Editor: Hanna Boogaard

Keywords:
Positive Matrix Factorization
Ultrafine particles
Particle number size distributions
Photonucleation
Traffic emissions
Airport emissions

ABSTRACT

Ultrafine particles (UFP) are suspected of having significant impacts on health. However, there have only been a limited number of studies on sources of UFP compared to larger particles. In this work, we identified and quantified the sources and processes contributing to particle number size distributions (PNSD) using Positive Matrix Factorization (PMF) at six monitoring stations (four urban background and two street canyon) from four European cities: Barcelona, Helsinki, London, and Zurich. These cities are characterised by different meteorological conditions and emissions. The common sources across all stations were *Photonucleation*, traffic emissions (3 sources, from fresh to aged emissions: *Traffic nucleation*, *Fresh traffic* – mode diameter between 13 and 37 nm, and *Urban* – mode diameter between 44 and 81 nm, mainly traffic but influenced by other sources in some cities), and *Secondary* particles. The *Photonucleation* factor was only directly identified by PMF for Barcelona, while an additional split of the *Nucleation* factor (into *Photonucleation* and *Traffic nucleation*) by using NO_x concentrations as a proxy for traffic emissions was performed for all other stations. The sum of all traffic sources resulted in a maximum relative contributions ranging from 71 to 94% (annual average) thereby being the main contributor at all stations. In London and Zurich, the relative contribution of the sources did not vary significantly between seasons. In contrast, the high levels of solar radiation in Barcelona led to an important contribution of *Photonucleation* particles (ranging from 14% during the winter period to 35% during summer). *Biogenic* emissions were a source identified only in Helsinki (both in the urban background and street canyon stations), that contributed importantly during summer (23% in urban background). Airport emissions contributed to *Nucleation* particles at urban background sites, as the highest concentrations of this source took place when the wind was blowing from the airport direction in all cities.

1. Introduction

It has been widely reported that atmospheric particulate matter (PM) has a negative impact upon human health, with 7 million deaths per year attributed to the exposure to air pollution (WHO, 2018). Disentangling the impact on public health of the different sources contributing to PM would allow targeted policies to reduce emissions. Sources of mass concentrations of PM $\leq$10 μm and $\leq$2.5 μm in

* Corresponding author.
E-mail address: ioar.rivas@isglobal.org (I. Rivas).

https://doi.org/10.1016/j.envint.2019.105345
Received 31 May 2019; Received in revised form 16 November 2019; Accepted 17 November 2019
Available online 04 December 2019

aerodynamic diameter (PM_{10} and $PM_{2.5}$, respectively) have been identified and quantified in different cities and regions around the world (e.g. Amato et al., 2016; Pancras et al., 2013; Viana et al., 2008; Wang and Shooter, 2005), but less is known about the sources and their contribution to ultrafine particle (UFP, particles ≤ 0.1 μm) number concentrations (PNC) (Vu et al., 2015). Previous studies suggest that sources dominating PNC differ from those dominating particle mass concentrations as detailed in Table S1 for the four European cities studied in this work. The quantification of the sources affecting UFP is very important as epidemiological studies suggest that negative health effects may be enhanced with decreasing particle size (Meng et al., 2013; Sioutas et al., 2005), although the associations between UFP and mortality or hospital admissions have been inconsistent in the literature (Kettunen et al., 2007; Lanzinger et al., 2016; Ohlwein et al., 2019; Samoli et al., 2016; Stafoggia et al., 2017; Tobías et al., 2018).

In urban areas, road traffic constitute the main source of UFP (Kumar et al., 2014; Morawska et al., 2008; Shi et al., 2001) but few attempts have been made to quantify its contribution to PNC (Beddows et al., 2015; Friend et al., 2012; Kasumba et al., 2009; Kim et al., 2004; Liu et al., 2014; Ogulei et al., 2006; Pey et al., 2009; Sowlat et al., 2016; Squizzato et al., 2019; Zhou et al., 2004, 2005). Emissions from vehicles are dependent upon the vehicle technology and the properties of fuels and lubricant oils, as well as the driving conditions (Jones et al., 2012; Kittelson et al., 2002; Lähde et al., 2009; Maricq et al., 2002; Rönkkö et al., 2017, 2014; Sgro et al., 2008). Primary particles in the vehicle exhaust include soot particles with mean particle around 30–100 nm (Kittelson, 1998; Maricq et al., 2002) and solid core particles in the nucleation mode, usually below 10–15 nm (Rönkkö et al., 2017, 2013; Sgro et al., 2008; Yao et al., 2005). Undiluted vehicle exhaust emissions, which are at very high temperatures, contain also a variety of different gaseous components, mainly volatile organic compounds (VOCs) and sulphuric acid. Since the saturation ratio of these gaseous compounds rises as the gas cools, these compounds either condense or nucleate to the particle phase immediately after the exhaust discharge to the atmosphere (Casati et al., 2007; Kittelson, 1998; Shi and Harrison, 1999). Which process predominates, condensation or nucleation, depends on the availability of pre-existing particle surface area (condensation sink; McMurry and Friedlander, 1979) along with the dilution and cooling rate (Morawska et al., 2008). Those nucleated particles have been named *delayed primary aerosols* by Rönkkö et al. (2017) since they are typically present in the particle phase in normal ambient air temperatures. Secondary particles are also generated from gaseous precursors from vehicle exhaust emissions when fully diluted within the ambient air and, driven by photochemistry, are oxidised by reactive species. This oxidation causes VOCs to turn into less volatile species, enhancing secondary aerosol formation by condensation and new particle formation (Gentner et al., 2012; Robinson et al., 2007; Volkamer et al., 2006).

Besides traffic, other sources are known to contribute to UFP. Ports and shipping emissions have been identified as source of UFP. Shipping emissions are characterised by high concentrations of VOCs and sulphur dioxide that result in the formation of secondary particles by nucleation and condensation processes (Kasper et al., 2007). Particle number size distributions (PNSD) from shipping emissions are characterised by an ultrafine mode with mode diameters ranging between 20 and 50 nm (Healy et al., 2009; Kasper et al., 2007). Sulphur content on shipping fuels has started to be controlled, with two areas in northern Europe in which sulphur emissions are tightly limited, including the Baltic Sea. Gas- (Brewer et al., 2016; Yu et al., 2018) and, specially, coal-fired power plants (Wang et al., 2011a) and airports (Cheung et al., 2011) are other relevant sources of ultrafine particles that may affect PNC in urban environment.

Ultrafine PNSD are complex. In contrast to the mass concentration, which is predominantly conservative, particles undergo several processes that modify their PNC and size such as new particle formation (nucleation), evaporation, condensation, deposition, and coagulation (Harrison et al., 2018). Therefore, freshly emitted particles may have a PNSD that may be transformed as these particles move away from the source (Zhu et al., 2002). Accordingly, primary particles would mainly influence the air quality near the emission source, while secondary particles would become more relevant as they travel away from the source to the urban background (UB; Morawska et al., 2008; Yao et al., 2005).

Therefore, there is a need for identification, characterisation, and quantification of the contribution of different sources contributing to PNC. Long-term measurements in different stations provide essential information for understanding the intricate relationship between local emission sources, particle atmospheric transformations, and meteorological processes. Numerous studies have investigated the effect on PNC and PNSD of specific sources in urban areas (Brines et al., 2015; Dall'Osto et al., 2013; Keuken et al., 2015; Zhu et al., 2002). However, long-term PNSD measurements are still scarce (Hofman et al., 2016; Pey et al., 2008; Reche et al., 2011b; Squizzato et al., 2019; Sun et al., 2019; Von Bismarck-Osten et al., 2013; Wang et al., 2011b) since UFPs are not a regulated pollutant. In addition, many different approaches are used to carry out source contribution analysis and direct comparison of results among studies is difficult. However, a number of source apportionment studies with Positive Matrix Factorization (PMF) applied to PNSD have been done before, mainly in the United States (Kim et al., 2004; Ogulei et al., 2007; Squizzato et al., 2019; Zhou et al., 2004) but also in China (Liu et al., 2014), Australia (Friend et al., 2012), and Europe (Czech Republic: Leoni et al., 2018; Germany: Yue et al., 2008; UK: Beddows et al., 2015).

The aim of this work is to identify sources and processes and quantify their contributions to urban ambient concentrations of PNC, by using the same methodological approach applied to long-term measurements of PNSD in four European cities with varying climatic and emission patterns: Barcelona, Helsinki, London, and Zurich.

2. Methodology

2.1. Monitoring stations

This study is based on data from four UB stations located in four European cities (Fig. 1; Table 1) with different climatic conditions, emission sources, and urban morphology. Two street canyon sites (one in Helsinki and one in London) were also evaluated to compare with the sources observed at the UB sites.

2.1.1. Barcelona (Urban Background)

Barcelona is located in the Northeast coast of Spain, in the western Mediterranean Basin. With 1.6 million inhabitants (3.6 million in its metropolitan area) in 2016 (Eurostat, 2018). Barcelona has one of the highest cars densities in Europe (5,500 registered cars km^{-2}; DGT, 2018), far above the traffic densities commonly observed in other cities across Europe (1,000–1,500 cars km^{-2}). The traffic fleet is characterised by a high proportion of diesel cars (40%) and buses (89% in 2015; DGT, 2018). Moreover, Barcelona holds one of the main harbours in the Mediterranean Basin, which may be a significant source of air pollutants that can be often carried by the sea breeze towards the city. The airport is located in a near city (about 10 km away from the monitoring station), with around 300,000 operations per year (AENA, 2018).

The measurements were carried out at the Palau Reial UB monitoring site (BCN, Table 1) located in southwest Barcelona that is influenced by vehicular emissions from one of the main traffic avenues of the city (at an approximate distance of 300 m) with an average traffic density of 70,000 vehicles/working day.

2.1.2. Helsinki (urban traffic and urban background)

Helsinki is a coastal city situated in southern Finland, at the shore of the Gulf of Finland. It is the largest city in Finland with 0.6

Fig. 1. Location of the cities under study: Barcelona (Spain), Helsinki (Finland), London (United Kingdom), and Zurich (Switzerland).

million inhabitants (1.1 million if considering the metropolitan area) in 2016 (Eurostat, 2018). Helsinki's car density is around 1,400 cars km^{-2} (Statistics Finland, 2018). On average, Finland had a share of diesel vehicles of 26.8% in 2016 (http://www.aut.fi/en/statistics/long-term_statistics/share_of_diesel_cars). Helsinki's port was the busiest passenger port in Europe in 2017 with 12.3 million passengers (Port of Helsinki, 2018). Ships crossing the Baltic Sea must run on fuel with low sulphur content (International Maritime Organization MARPOL regulation). The airport has around 85,000 landings per year (FINAVIA, 2018) and it is about 13 km N from the UB station (HSK).

The SMEAR III (Station for Measuring Ecosystem–Atmosphere Relationships) UB station in Kumpula, Helsinki (HSK, Table 1), is located in an area with different urban land uses varying from allotment gardens to office areas (e.g. University of Helsinki) and single family house areas with relatively low traffic loads. The station is close (about 200 m) to one of the main roads to the city centre with an average traffic density of 50,000 vehicles/day (Järvi et al., 2009).

The traffic-monitoring site in Helsinki is adjacent to Mäkelänkatu and can be classified as a street canyon (HSK_SC, Table 1) with a traffic density of 28,000 vehicles/working day. In its 42 m of width, Mäkelänkatu has six lanes with two tramlines and rows of trees in the middle. The road is flanked by four- and five-storey buildings (height-to-width ratio of 0.4; Rönkkö et al., 2017). HSK_SC is located about 870 m southwest of the HSK site.

2.1.3. London (urban traffic and urban background)

London is in southeastern England (UK). Greater London has 8.7 million inhabitants, making it the largest city in the European Union (Eurostat, 2018). Car density in London is around 1,700 cars km^{-2}. In 2015, the proportion of diesel cars in the urban areas of England was of 46% in vehicles-kilometres (number of vehicles on a traffic network multiplied by the average length of their trips measured in kilometres, as measure of traffic flow) and the proportion of diesel buses in London was 83% vehicle-kilometres (UK NAEI, 2014). London is surrounded by several airports, some of them over 30 km away. The busiest is Heathrow with around 480,000 movements/year in 2018 and is located approximately 18 km from the UB station at North Kensington.

The North Kensington UB monitoring station (LND, Table 1) is placed in the grounds of Sion Manning School in St Charles Square and is mainly a residential area. The London traffic monitoring station (LND_SC, Table 1) is sited in the kerbside of Marylebone Road, one of the most heavily trafficked of the city with over 80,000 vehicles/working day. It is a street canyon with six lanes (height-to-width ratio of 0.8) that experiences frequent congestion. The LND_SC station is about 4 km to the east of the LND station. Both stations belong to the London Air Quality Network.

Table 1
Information about the monitoring stations selected for the study.

City (country)	Station	Sation ID	Station type	Coordinates	Busiest traffic hour* (local time, h)
Barcelona (ES)	Palau Reial	BCN	Urban Background	41° 23′ 14″ N, 02° 06′ 56″ E, 80 m a.s.l.	Morning: 8–9 Evening: 18–19
Helsinki (FI)	Mäkelänkatu	HSK_SC	Urban traffic – street canyon	60°11′47″N, 24°57′08″E, 32 m a.s.l.	Morning: 8–9
Helsinki (FI)	SMEAR III Kumpula	HSK	Urban Background	60° 12′ 11″ N, 24° 57′ 40″ E, 24 m a.s.l.	Evening: 16–17
London (GB)	Marylebone	LND_SC	Urban traffic – street canyon	51° 31′ 21″ N, 00° 09′ 17″ W, 35 m a.s.l.	Morning: 8–9
London (GB)	North Kensington	LND	Urban Background	51° 31′ 16″ N, 00° 12′ 48″ W, 27 m a.s.l.	Evening: 17–18
Zurich (CH)	Kaserne	ZRC	Urban Background	47° 22′ 39″ N, 8° 31′ 50″ E, 409 m.a.s.l.	Morning: 7–8 Evening: 17–18

* Peak hours were obtained from the TomTom© Traffic Index (https://www.tomtom.com/en_gb/trafficindex/).

Meteorological parameters for both stations were obtained at Heathrow Airport, including solar radiation (UK Met Office, 2006).

2.1.4. Zurich (urban background)

Zurich is located in northeastern Switzerland and is the smallest of the cities in this study. The city of Zurich has 0.4 million inhabitants (0.6 million including the metropolitan area) and a car density of 2,000 vehicles km^{-2}. In Switzerland, and presumably also in Zurich, the vehicle fleet consists of 27.2% diesel vehicles, 71.2% gasoline vehicles and 1.6% hybrid and electrical powered vehicles (BFS, 2016).

The measurements were carried out at the Zurich-Kaserne UB station (ZRC, Table 1) that is part of the Swiss National Air Pollution Monitoring Network (NABEL). It is located in a public courtyard in the city centre. The roads surrounding the station have low traffic intensity and the area is not affected by major emissions from industries but it is close to a district with high density of restaurants (west). The biggest train station in Switzerland is located about 300 m away northeast. Zurich airport, with around 270,000 movements per year, is located 10 km north. There is a military base (converted to a civil airport with joint military use in 2014) with very little volume of air traffic. It is located 9 km NE from the monitoring station.

2.2. Instrumentation

The instrumentation used for measuring aerosol and gaseous pollutants at the different stations is described in Table 2. For the present study, the data were averaged to hourly values. The periods under study varied depending on the data availability for each site (from 2007 to 2017). Different instruments and measuring configurations were used for PNSD measurements at the different sites, and, thus, the measured size ranges varied: in BCN from 11 to 478 nm (Scanning Mobility Particle Sizer Spectrometer, SMPS TSI 3936), in HSK from 6 to 700 nm (Differential Mobility Particle Sizer, DMPS), in HSK_SC from 6 to 800 nm (DMPS), in LND and LND_SC from 17 to 604 nm (SMPS TSI 3080), and in ZRC from 10 to 487 nm (SMPS TSI 3034). Most of the instruments for measuring PNSD were fitted with a dryer (except the one in Barcelona and Zurich) as recommended by the EUSAAR protocol (Wiedensohler et al., 2012) and were corrected for diffusional losses (except in Zurich). These differences, particularly in the lower size cut, complicate the comparison of the number concentration of smallest particle and total PNC. The SMPS and DMPS underwent several checks for quality control and assurance. On a daily basis, all instruments were checked to ensure they were turned on and working correctly. The impactors and inlets were cleaned on a weekly or biweekly basis. Flow rates were measured at least once a month (twice a month at most of the stations) to ensure the flow was within ± 10%. Once per year, the instruments were either sent for complete maintenance (and the high-voltage supply of the DMA was checked) or participated in a calibration workshop with other SMPS or DMPS (e.g. Gómez-Moreno et al., 2015).

Black Carbon (BC), PM mass (except HSK), and gaseous pollutant (NO_2, NO, SO_2, CO, O_3) concentrations were also monitored (Table 2). The instruments for BC and PM monitoring were also checked frequently: the impactors were cleaned at least once per month and the concentrations were compared to gravimetric measures for PM and elemental carbon determinations for BC. Flow is very stable for both types of instruments and were checked at least twice per year in all cities. Both PM and gaseous monitoring are performed according to the European Union standards (Directive 2008/50/EC).

2.3. Positive Matrix Factorisation (PMF)

Positive Matrix Factorisation (PMF; Paatero, 1997) is a widely used multivariate data analysis method to identify and apportion the sources of PM or PNSD by analysing the measurements of observed species (or size bins in the case of PNSD) at the receptor site. PMF is a least-squares method that assumes that ambient aerosol X (a matrix of $n \times$ observations and $m \times$ size bins) can be explained by the product of a source matrix F and a contribution matrix G, whose elements are given by Eq. (1):

$$x_{ij} = \sum_{k=1}^{p} g_{ik} \cdot f_{jk} + e_{ij} \quad (1)$$

where p is the number of independent sources, X_{ij} is the measured submicron particle number concentration of the *jth* size bin in the *ith* sample, f_{jk} is the concentration of the *jth* size bin in material emitted by source k, g_{ik} is the contribution of the kth source to the *ith* sample, and e_{ij} represents the residuals.

PMF is a descriptive model and there are no objective criteria with which to choose the best solution. PMF was performed with Multilinear Engine 2 (ME-2, Paatero, 1999), to identify and quantify the sources of PNSD. ME-2 was used instead of the USEPA PMF 5.0 because the latter software accepts a limited number of observations. The hourly averaged PNSD data were combined with the hourly concentrations of gaseous pollutants (NO_2, NO, SO_2, CO, O_3). Adding additional species (other than PNSD) can help to separate and identify the sources. It can also decrease the rotational ambiguity because of increased numbers of edge points (Emami and Hopke, 2017; Li et al., 2019). BC was not included in the PMF analyses because the data coverage was low for some of the stations. However, we performed a sensitivity analysis (data not shown) to test the influence of including BC in the factor profiles and contributions and we obtained very similar results. PM mass concentrations were also excluded for three reasons: (1) because they were not available for HSK, (2) ultrafine particles contribute very little to PM mass concentrations and are generally uncorrelated with them, and (3) several different sources may be affecting PM mass concentrations and, thus, the mass values may not add useful source information to PMF as PM composition data would. Although CO and SO_2 were not available for HSK_SC, these species were used for the other sites because UB stations are the focus of this study and the HSK_SC dataset only covered a short period.

PMF requires individual uncertainty estimates for each data value. We followed the methodology established by Ogulei et al. (2007) with little variations. The following equation was used to calculate the measurement uncertainties:

$$\sigma_{ij} = \alpha_j \cdot (N_{ij} + \bar{N}_j) \quad (2)$$

where σ_{ij} is the estimated measurement error for size bin or gaseous pollutant j and sample i; α_j is a constant for size bin or gaseous pollutant j; N_{ij} is the observed concentration for size bin or gaseous pollutant j and sample i; and $\bar{N}_j$ is the arithmetic mean of the observed concentration for size bin or gaseous pollutant j. We tested values of α between 0.005 and 0.030. Selected α are presented in Table S2. Commonly, α is used as a constant throughout all size bins and pollutants, however, we added higher uncertainty to the lowest and the highest bins of the PNSD as they have been reported to have increased measurement error (Wiedensohler et al., 2018). Thus, we assigned $2^*\alpha$ for the 3% lowest and 3% highest size bins (we had different instruments with different number of bins), and $1.5^*\alpha$ for the subsequent 3% lower and 3% higher size bins. Afterwards, we fitted a spline and used the modelled values as the α_j for the PNSD. For the gaseous pollutants, we used a scaling factor (multiplier) of 4 for α which was empirically determined to adjust the distribution of scaled residuals between the reasonable range of −3 and 3 (see below).

The overall uncertainty matrix was calculated as:

$$s_{ij} = \sigma_{ij} + C_3 \cdot N_{ij} \quad (3)$$

where σ_{ij} is the estimated measurement error (Eq. (2)) and C_3 is a constant. Both α and C_3 were chosen so (1) the scaled residuals were approximately randomly distributed between −3 and 3, (2) the model obtained closest value of the object function (Q, sum of scaled residuals) to the theoretical value, and (3) provided the most physically

Table 2
Instrumentation used to monitor particles at the different monitoring stations.

Station	PNC (pt cm^{-3})	PNSD (pt cm^{-3})	BC (μg m^{-3})	PMx (μg m^{-3})	Periods of study
BCN	WCPC[a] TSI models 3785 and 3787 (N_{5-1000})	SMPS[b] TSI 3936. Electrostatic Classifier TSI 3080 + DMA[c] TSI 3081 + CPC[d] TSI 3772),(N_{11-478})	MAAP[e] Thermo ESM Andersen Instrument with PM_{10} inlet	PM optical counters GrimmLabortechnik GmbH& Co. models 180.	January 2013 – December 2016
HSK_SC	N data from DMPS (N_{6-800})	DMPS[f] (Airmodus CPC A20 and Vienna type DMA) (N_{6-800})	MAAP[e] Thermo ESM Andersen Instruments with PM_1 inlet	TEOM[g] 1405	February 2015 – August 2017
HSK	CPC 3022 ($N_{10-1000}$) Since March 2013: Airmodus A20 CPC (N_{7-1000})	DMPS[f], Hauke-type DMA[c], 10.9 cm + CPC[d] TSI 3025; Hauke-type DMA[c], 28 cm + CPC[d] TSI 3010), (N_{6-700})	RT-OCEC, Sunset Lab, with PM_1 inlet	–	January 2007 – December 2016
LND	CPC TSI 3022A (N_{7-1000})	SMPS[b] TSI Electrostatic Classifier TSI 3080 + DMA[c] TSI 3081 + CPC[d] TSI 3775), (N_{17-640})	Aethalometer AE21 (Magee Scientifc)	TEOM[g]-FDMS[h] 1405F (Thermo Scientific)	January 2010 – December 2016
LND_SC	CPC TSI 3022A (N_{7-1000})	SMPS[b] TSI Electrostatic Classifier TSI 3080 + DMA[c] TSI 3081 + CPC[d] TSI 3775), (N_{17-640})	Aethalometer AE21 (Magee Scientifc)	TEOM[g]-FDMS[h] 1405F (Thermo Scientific)	March 2014 – December 2016
ZRC	CPC[d] 3775 (N_{4-3000})	SMPS[b] TSI 3034 + Nafion aerosol dryer ($_{N10-487}$)	Aethalometer AE31 (Magee Scientifc)	TEOM[g] 8500 FDMS[h] (Thermo Scientific)	December 2010 – October 2014

[a] Water-based condensation particle counter.
[b] Scanning mobility particle sizer spectrometer.
[c] Differential mobility analyzer.
[d] Condensation particle counter.
[e] Multi-angle absorption photometer.
[f] Differential mobility particle sizer.
[g] Tapered element oscillating microbalance.
[h] Filter dynamics measurement system.

interpretable results. Thus, as for α, C_3 was empirically determined through a trial-and-error approach by testing values between 0.05 and 0.15 (values of C_3 optimising the model are presented in Table S2).

Only when missing values corresponded to less than 25% of the number of size bins and gaseous pollutants within a timestamp (that is, at least 75% of the variables had data available), we imputed the concentrations. If no data were available for any PNSD size bin during a specific timestamp, it was excluded from the analysis. The missing cells within included observations were imputed using the 'mice' (Multivariate Imputation by Chained Equations) R package (Van Buuren and Groothuis-Oudshoorn, 2011). The corresponding uncertainties for imputed data were set to twice the imputed value.

The PNSD source profiles and contributions obtained from the ME-2 analyses were scaled to the measured concentration by regressing the measured total PNSD against the ME-2 contribution matrix.

We performed the analyses to all-year dataset. Previous literature suggest performing the analyses by season to account for the substantial season-to-season variability in temperature and solar radiation (Ogulei et al., 2007). We compared all-year results with the results obtained when performing PMF separately by season: summer (June, July, and August), winter (December, January, and February) and transitional period (March, April, May, September, October, and November). We obtained the same number of sources and most of them showed a correlation coefficient > 0.98. However, some differences were observed for specific sources, as shown by some goodness-of-fit measures (Table S3). These differences were mainly due to transfer of contributions between two sources (often of the same nature such as two traffic sources) for one of the seasons during the year. For some stations, carrying out a PMF for each season led to inexplicable strong jumps in the source contributions from the last day of a season to the first of the following season). Thus, we selected to present the results of the all-year dataset as it captured a smoothed season-to-season variability and ensured continuity of the sources throughout the year.

2.4. Statistical software

Data management, descriptive statistics, and plots were performed with the R statistical software (v 3.5.1., R Core Team, 2018) and the package *openair* (Carslaw and Ropkins, 2012).

3. Results and discussion

Summary statistics for the different pollutants and meteorological data are presented in Table 3 for all monitoring stations. PM_{10}, $PM_{2.5}$ and NO_2 average concentrations were below the European limit values of 40, 25, and 40 $\mu g\ m^{-3}$ (annual average), respectively, in UB stations from all cities. PNC and PNSD are difficult to compare between stations, as the measurement protocol and, specially, the measured particle size differs considerably. To quantify the effect of the differences in the size ranges, we calculated the total PNC for a reduced common range of approximately 17–480 nm (Table S4) and resulted in a reduction of 45% of the full PNSD range for HSK_SC, 27% for HSK, 26% for ZRC, 17% for BCN with almost the same concentration for the London stations. Thus, when interpreting the source contributions, we should take into account these differences and that these differences will affect mainly the sources in the nucleation mode. Concentrations of BC and the gaseous pollutants that are tracers of combustion processes were highest at the London stations (and particularly the traffic station, LND_SC), followed by HSK_SC, BCN, ZRC, and finally, with the lowest concentrations, the UB station of HSK. The average temperature over the measurement period were lowest in Helsinki, followed by similar temperatures in London and Zurich, and the highest being in Barcelona. As expected, solar radiation increased from north to south, with the lowest average being observed in Helsinki and the maximum in Barcelona.

The datasets for each site were independently analysed by PMF. Those PMF solutions that had the most physically meaningful profile and temporal behaviour were selected after comparing solutions with different number of factors (Ogulei et al., 2007; Vu et al., 2015). The factors that were common in the different stations, although with slightly different profiles, were *Nucleation*, two traffic factors (*Fresh traffic* and *Urban*, the latter dominated by traffic emissions but influenced by other urban sources including biomass burning in some cities during the cold periods), and *Secondary* aerosol. In addition, in Helsinki *Biogenic* contributions were identified as a separated factor (further details in the sources below). For all stations PMF predictions of PNSD correlated very well with the observed values (Fig. S1). For BCN, new particle formation through photonucleation processes had such a high impact that *Photonucleation* was separated by PMF as a differentiated factor from nucleation particles emitted by road traffic (and nucleation particles from traffic exhaust were included in the *Fresh traffic* factor, which was specifically labelled as *Traffic (nucleation + fresh)* for the BCN site). At the other stations, however, the low correlation between traffic tracers such as BC and NO_x and the *Nucleation* factor indicated that *Nucleation* also included particles generated by photonucleation processes, as there were high concentrations of the *Nucleation* source under low NOx concentration conditions (Fig. S2).

3.1. Splitting of the Nucleation factor into Photonucleation and Traffic Nucleation sources

We developed a methodology (inspired by the one proposed by Rodríguez and Cuevas, 2007) to split the *Nucleation* factor into two sources: *Photonucleation* and *Traffic nucleation*. To this end, we used NO_x as a proxy for traffic emissions within the *Nucleation* factor. Considering that at the morning peak hour most of the Nucleation particles would be from traffic, we multiplied NO_x concentration by a scaling factor (the ratio between *Nucleation* and NO_x) so it matched *Nucleation* concentrations at morning peak hour (08:00 h local time, except for HSK_SC that was at 07:00 h). The scaling factor was different for each day (day-specific) to account for the possible variations in the NO_x to *Nucleation* ratio due to: (1) long-term changes in the fleet (differences in the fuel proportion and the emission control technologies incorporated in the vehicles; Park et al., 2017; Rönkkö et al., 2013); (2) driving conditions (Wang et al., 2010); and (3) the dependency on meteorological and dilution conditions of particle formation (affecting to nucleation particles) in diluting engine exhaust (Charron and Harrison, 2003; Gidhagen et al., 2005; Rönkkö et al., 2006). For daytime hours (from 08:00 to 21:00 h local time), if solar radiation was over 10 W/m^2, the product of hourly NO_x concentrations by the day-specific factor was assigned to the *Traffic nucleation* source, while the rest was assumed to be *Photonucleation* (*Photonucleation = Nucleation – Traffic nucleation*; Fig. S2). During the night (22 h – 07:00 h) all *Nucleation* particles were assigned to *Traffic nucleation* as no photonucleation would be expected. In this work, we use the term 'factor' when referring to the direct results from PMF (e.g. for the profile description) and the term 'source' when discussing about the final sources after the splitting of the *Nucleation* factor.

3.2. Traffic size distributions

Regarding the different traffic factors (including the one labelled as *Urban*) identified at each station, the profiles obtained from this work (Fig. 2) are within those reported at the existing literature. As stated in the reviews by Morawska et al. (2008) and Vu et al. (2015), diesel exhaust emissions are within the size range of 10–130 nm while gasoline emissions are within 15–60 nm. Exhaust plumes are characterised by the emission of primary particles (a carbonaceous mode) and secondary nucleation particles (Morawska et al., 2008). Exhaust primary particles are within the range of 30–500 nm (Casati et al., 2007; Vu et al., 2015) and are mainly composed of agglomerates of solid carbonaceous material (soot: graphitic carbon and lesser quantities of

Table 3
Average (and standard deviation) of pollutant concentrations and weather variables for the periods of study (only for periods when simultaneous PNSD and NO_x data was available). For wind direction, the most frequent direction from where the wind was blowing is indicated.

Station	PNCcpc (pt cm^{-3}) *	PNSD (pt cm^{-3})¤	BC (μg m^{-3})	$PM_{2.5}$ (μg m^{-3})	PM_{10} (μg m^{-3})
BCN	$PNC_{5\text{-}1000}$: 11709 (7477)	$PNC_{11\text{-}478}$: 11343 (7518)	1.1 (1.0)	15.8 (8.6)	23.5 (12.9)
HSK	$PNC_{10\text{-}1000}$ ($PNC_{7\text{-}1000}$ since March 2013): 5653 (4351)	$PNC_{6\text{-}800}$: 7003 (5498)	0.53 (0.55)	–	–
HSK_SC		$PNC_{6\text{-}800}$: 15482 (13208)	1.3 (1.2)	7.9 (5.0)	21.8 (21.9)
LND	$PNC_{7\text{-}1000}$: 10211 (6501)	$PNC_{17\text{-}640}$: 5630 (3600)	1.4 (1.4)	13.8 (11.5)	21.1 (13.4)
LND_SC	$PNC_{7\text{-}1000}$: 17269 (9452)	$PNC_{17\text{-}640}$: 12328 (6663)	5.5 (3.8)	16.8 (10.9)	25.4 (14.0)
ZRC	$PNC_{4\text{-}3000}$: 12835 (7581)	$PNC_{10\text{-}487}$: 9487 (6797)	0.88 (0.74)	–	17.3 (13.1)
Station	**NO_2 (μg m^{-3})**	**NO (μg m^{-3})**	**CO (mg m^{-3})**	**SO_2 (μg m^{-3})**	**O_3 (μg m^{-3})**
BCN	31.9 (23.5)	9.4 (23.8)	0.32 (0.19)	2.0 (1.5)	54.7 (28.7)
HSK	17.7 (16.9)	4.1 (15.7)	0.26 (0.08)	1.9 (3.3)	49.1 (21.8)
HSK_SC	38.0 (24.1)	33.9 (44.5)	–	–	37.4 (19.4)
LND	34.8 (21.3)	19.3 (50.0)	0.26 (0.15)	2.0 (2.2)	38.9 (25.7)
LND_SC	90.0 (41.0)	214 (176)	0.51 (0.27)	8.4 (4.4)	15.0 (13.3)
ZRC	30.3 (18.7)	10.5 (21.7)	0.31 (0.15)	2.0 (2.2)	47.6 (34.5)
Station	**Temperature (°C)**	**Relative Humidity (%)**	**Wind speed (m s^{-1})**	**Wind direction (°)**	**Solar radiation (W m^{-2})**
BCN	18.2 (5.9)	70.9 (14.5)	2.0 (1.4)	280	180 (267)
HSK	6.7 (9.0)	74.9 (16.3)	4.2 (1.9)	230	114 (195)
HSK_SC	8.5 (8.0)	70.7 (14.2)	1.2 (0.75)	300	124 (202)
LND	11.8 (6.0)	76.4 (15.6)	4.0 (2.1)	220	122 (198)
LND_SC	12.3 (5.6)	76.2 (15.8)	4.1 (2.2)	220	126 (201)
ZRC	12.2 (7.9)	69.0 (15.8)	2.0 (1.3)	320	140 (225)

Periods of study:
BCN: January 2013 - December 2016; HSK_SC: February 2015 – August 2017; HSK: January 2007 – December 2016; LND_SC: March 2014 – December 2016; LND: January 2010 – December 2016; ZRC: December 2010 – October 2014.

metallic ash with condensed or adsorbed hydrocarbons and sulphur compounds). The carbon core diameter has been reported to be down to 2.5 nm in cars (Sgro et al., 2008) and 10 nm in heavy-duty vehicles (Rönkkö et al., 2013). Heavy-duty vehicles may also emit coarser primary particles within the accumulation mode (100–1000 nm; Morawska et al., 1998). Nucleation particles form from the hot exhaust gases while they cool down and condense to produce large numbers of particles in the nucleation range (< 30 nm) (Morawska et al., 2008). Binary nucleation of H_2SO_4-H_20 or ternary nucleation of H_2SO_4-NH_3-H_2O are the main mechanisms of particle formation (Meyer and Ristovski, 2007; Shi and Harrison, 1999). The small sulphuric acid core starts growing by condensation of hydrocarbons (Tobias et al., 2001). In this study, the mode diameters of the profiles of the different traffic factors fall within the abovementioned size ranges (Table 4). The *Nucleation* factors showed a size range of 7–21 nm and, thus, traffic nucleation particles may be the principal contributor. The lower size range is especially dependent on the lower size-cut of the instrument used for PNSD measurements but in all cities a source with a mode diameter below 25 nm was resolved (Table 4). The size range of mode diameters for *Fresh traffic* (14–37 nm) may correspond to fresher traffic emissions of core carbon particles with organic compounds condensed and absorbed, including smaller carbon agglomerates. *Urban* encompassed larger carbon agglomerates (as supported by the correlation of BC and *Urban* always being higher than for *Fresh traffic* and *Traffic nucleation*; Table S5) as well as aged traffic particles that had grown enough to be in this size-range. The latter was corroborated by the daily patterns of *Urban* concentrations that usually showed a longer and delayed peak in comparison with *Fresh traffic* (Fig. 3).

3.3. Sources in Barcelona (BCN)

Four factors were identified for BCN site. The profiles of the factors are presented in Fig. 2, both for the PNSD and gaseous data. The sources identified from the profiles were *Photonucleation* (size mode diameter: 13 nm), fresh traffic with a size mode of 31 nm but also including nucleation particles (labelled as *Traffic(nucleation + fresh)*), a second traffic source mixed with urban background emissions with a size mode of 76 nm (*Urban*, mostly traffic emissions but slightly influenced by other urban emissions), and *Secondary* particles with the coarsest particle size (mode: 175 nm; Table 4). The *Secondary* source showed a bimodal distribution, with a minor peak at 18 nm. A bimodal distribution was also observed by Pey et al. (2009) in BCN by using a completely different approach. Pey et al. (2009) observed a minor peak in the 23–30 nm and a major one at 310–800 nm, with a much higher contribution of the accumulation mode than the nucleation. The bimodal distribution of secondary aerosols has also been observed in other locations (e.g. Gu et al., 2011; Kasumba et al., 2009; Squizzato et al., 2019). Pey et al. (2009) attributed the secondary source to consist mainly of accumulation mode ammonium-sulphate and ammonium nitrate particles. The profiles for the gaseous pollutants also support the source identifications from the size distribution (Fig. 2): *Photonucleation* and *Secondary* particles were explained by high contributions from O_3, while the traffic sources were associated with high NO_2.

Although photonucleation particles were successfully separated from traffic nucleation particles by PMF in Barcelona, the minor peak at midday and the correlation between NO_x and *Traffic (nucleation + fresh)* (Fig. S3) suggested that the *Traffic nucleation* factor still included particles generated by photonucleation processes. Following the same methodology detailed above for the splitting of the *Nucleation* source in the other stations, the difference between the *Traffic (nucleation + fresh)* and the NO_x* factor was assigned to be photonucleation particles. These residual photonucleation particles were added to *the Photonucleation* source and subtracted from *Traffic (nucleation + fresh)*. With the exception of the source profile, all results presented in this work include the correction for the *Photonucleation* and *Traffic (nucleation + fresh)* sources.

The daily, weekly, and monthly patterns for each source are shown in Fig. 3 and were inspected to determine the correspondence with the source identifications. *Traffic (nucleation + fresh)* and *Urban* showed a daily pattern coinciding with the typical traffic peaks (Table 1). *Traffic (nucleation + fresh)* had an average annual contribution of 5207 ± 5468 pt cm^{-3} (Table 5) and showed the lowest concentrations

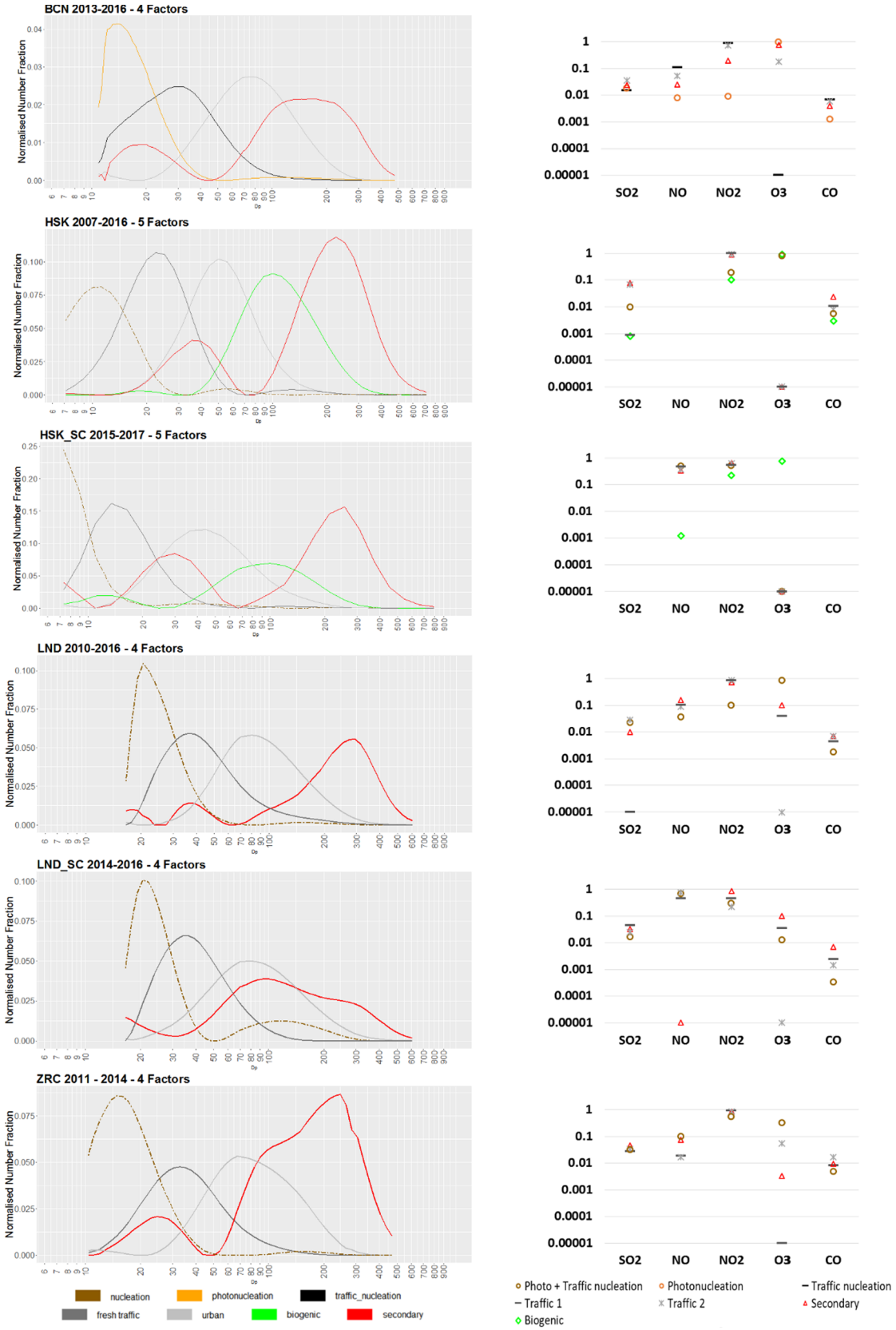

Fig. 2. Profiles of the sources including particle size distribution and gaseous species.

Table 4
Count median and mode diameter of the profile from the different sources.

	Count median diameter[a]					Mode diameter[b]				
	Nucleation*	Fresh traffic*	Urban	Secondary	Biogenic	Nucleation*	Fresh traffic*	Urban	Secondary	Biogenic
BCN* $PNC_{11\text{-}478}$	17.9	28.9	75.1	105.3	–	13.1	31.1	76.4	174.7	–
HSK $PNC_{6\text{-}800}$	11.8	22.9	51.0	148.1	106.1	11.2	22.4	50.1	224	100
HSK_SC $PNC_{6\text{-}800}$	8.6	15.7	45.5	91.2	74.7	7.33	13.4	44.7	256.3	99.9
LND $PNC_{17\text{-}640}$	25.7	44.5	90.2	178.8	–	20.6	36.6	80.6	294.3	–
LND_SC $PNC_{17\text{-}640}$	31.9	39.3	83.9	113.3	–	20.6	34.0	80.6	93.1	–
ZRC $PNC_{10\text{-}487}$	17.9	35.1	80.3	135.2	–	14.9	32.8	67.3	245.8	–

Periods of study:
BCN: January 2013 - December 2016; HSK_SC: February 2015 – August 2017; HSK: January 2007 – December 2016; LND_SC: March 2014 – December 2016; LND: January 2010 – December 2016; ZRC: December 2010 - October 2014.

* For Barcelona, 'Nucleation' corresponds to the 'Photonucleation' factor, and 'Fresh traffic' is the 'Traffic (nucleation + fresh)' factor.

[a] Count Median Diameter (CMD): $CMD = (D_1^{n1}D_2^{n2}D_3^{n3}\ldots D_k^{nk})^{1/N}$ where: D_i = midpoint particle size; n_i = number of particles in group *i* having midpoint size D_i; N = total particle number, summed over all size bins.

[b] Mode diameter: corresponds to the midpoint particle size in the bin with the highest PNC.

during the summer months (summer average: 3556 ± 2977 pt cm^{-3}) and the highest during late autumn (autumn average: 6223 ± 6330 pt cm^{-3}). The daily patterns by season are presented in Fig. S4. Similarly, *Urban* showed the lowest concentrations during August (2352 ± 1186 pt cm^{-3}), although the concentrations were more constant throughout the year (2835 ± 2103 pt cm^{-3}) than for *Traffic (nucleation + fresh)* due to the contribution of other urban background sources. Both sources related to traffic were greatest during weekdays and showed the least concentrations on Sunday. Moreover, *Traffic (nucleation + fresh)* and *Urban* showed high correlation with BC (r = 0.76 and r = 0.83, respectively; Table S5). *Photonucleation* showed a peak around midday, coinciding with the greatest levels of solar radiation (r = 0.51, Table S5), with negligible contributions during nighttime. *Photonucleation* also showed a small peak at 07:00 of misclassified particles that probably correspond to traffic emissions. *Photonucleation* did not show a consistent weekly pattern, with similar concentrations throughout the week. Contributions were minimal during the winter months (1506 ± 2690 pt cm^{-3}, average for 12–14 solar h: 3049 ± 2989 pt cm^{-3}) with significant contributions from June to August (3743 ± 5536 pt cm^{-3}, average for 12–14 solar h: 9153 ± 8554 pt cm^{-3}). The *Secondary* source (675 ± 572 pt cm^{-3}) seems to be influenced by traffic emissions since the morning peak and the greatest contributions on Fridays could be seen in the daily and weekly pattern. The correlation coefficient with BC is moderate (r = 0.58). The contributions from the *Secondary* from our study is much lower than the 2000–6000 pt cm^{-3} reported by Pey et al. (2009) for BCN in 2004 determined by means of Principal Component Analysis, however, sulphate levels were reduced by a large proportion since 2009 to the study period of this work (Pandolfi et al., 2016).

3.4. Sources in Helsinki (HSK and HSK_SC)

Five factors were identified for Helsinki: *Nucleation* (mode = 11 nm), *Fresh traffic* (22 nm), *Urban* (50 nm), *Biogenic* (100 nm), and *Secondary* (224 nm). The same factors were identified in the street canyon site, HSK_SC. However, at the HSK_SC the size modes were shifted towards smaller particles due to the proximity to the source for *Nucleation* (7 nm), *Fresh traffic* (13 nm), and *Urban* (45 nm). Although the *Biogenic* was characterised by the same size mode (100 nm) in both stations, the *Secondary* showed slightly larger particles (256 nm) at HSK_SC than at HSK (Table 4). Similar to BCN, the *Secondary* source also showed a bimodal distribution at both Helsinki stations with the minor peak being at around 33 nm in HSK and 30 nm in HSK_SC (Fig. 2). As indicated previously, the *Nucleation* source was split into *Photonucleation* and *Traffic Nucleation* (Fig. S2). The gaseous profiles indicate high contributions of NO_2 to the traffic sources (including the mixed source of *Photonucleation* and *Traffic Nucleation*) in both stations (Fig. 2). O_3 was mainly associated with the *Biogenic* source.

The daily and weekly concentration patterns corroborate the source identifications from the PNSD profiles (Fig. 3). Wood combustion contributed to *Urban* and also to *Fresh traffic* during winter, which, besides boundary layer height evolution over the year, would partly explain the higher contributions during the cold periods (Fig. S4; Ripamonti et al., 2013). Nevertheless, the main source of UFP number concentrations would still be traffic in HSK and especially in HSK_SC. In fact, in HSK_SC, BC attributed to biomass burning was 14% of total BC concentrations (Helin et al., 2018). The average annual concentrations were 1391 ± 1482 pt cm^{-3}, 1871 ± 2546 pt cm^{-3}, and 2219 ± 2269 pt cm^{-3} in HSK and 2811 ± 4050 pt cm^{-3}, 5636 ± 7056 pt cm^{-3}, and 4156 ± 3884 pt cm^{-3} in HSK_SC for *Traffic Nucleation*, *Fresh traffic*, and *Urban*, respectively (Table 5; refer to Table S6 for average contributions over the same period at HSK and HSK_SC). Regarding the *Biogenic* and *Secondary* sources, they did not present a specific daily or weekly pattern, with similar levels throughout the day and the week (Fig. 3). Annual averages were 1001 ± 923 pt cm^{-3} for *Biogenic* and 198 ± 219 pt cm^{-3} for *Secondary* in HSK and 1734 ± 1439 pt cm^{-3} and 226 ± 217 pt cm^{-3} in HSK_SC, respectively. However, the annual pattern showed important differences between these two sources. *Biogenic* had its peak during the warmer months (Fig. 3) when biogenic emissions (e.g. monoterpenes, isoprene) were at their maximum (Rantala et al., 2016). Biogenic VOC emissions are important precursors for new particle formation (Kirkby et al., 2016; Yan et al., 2018), which may reach the urban environment after they have grown up to around 100 nm. Although biogenic VOC emissions peak in summer, the frequency of new particle formation events is more common during spring and autumn due to the inhibition of new particle formation under high isoprene concentrations (Kiendler-Scharr et al., 2009) and because in cooler temperatures the particle-phase might be favoured by supersaturation. Since we observed the highest concentrations during summer, the *Biogenic* source may also have the input of particles from polluted air masses from long range transport, which is particularly intense in the summer months due to controlled burning and forest fires from other regions in Eastern Europe

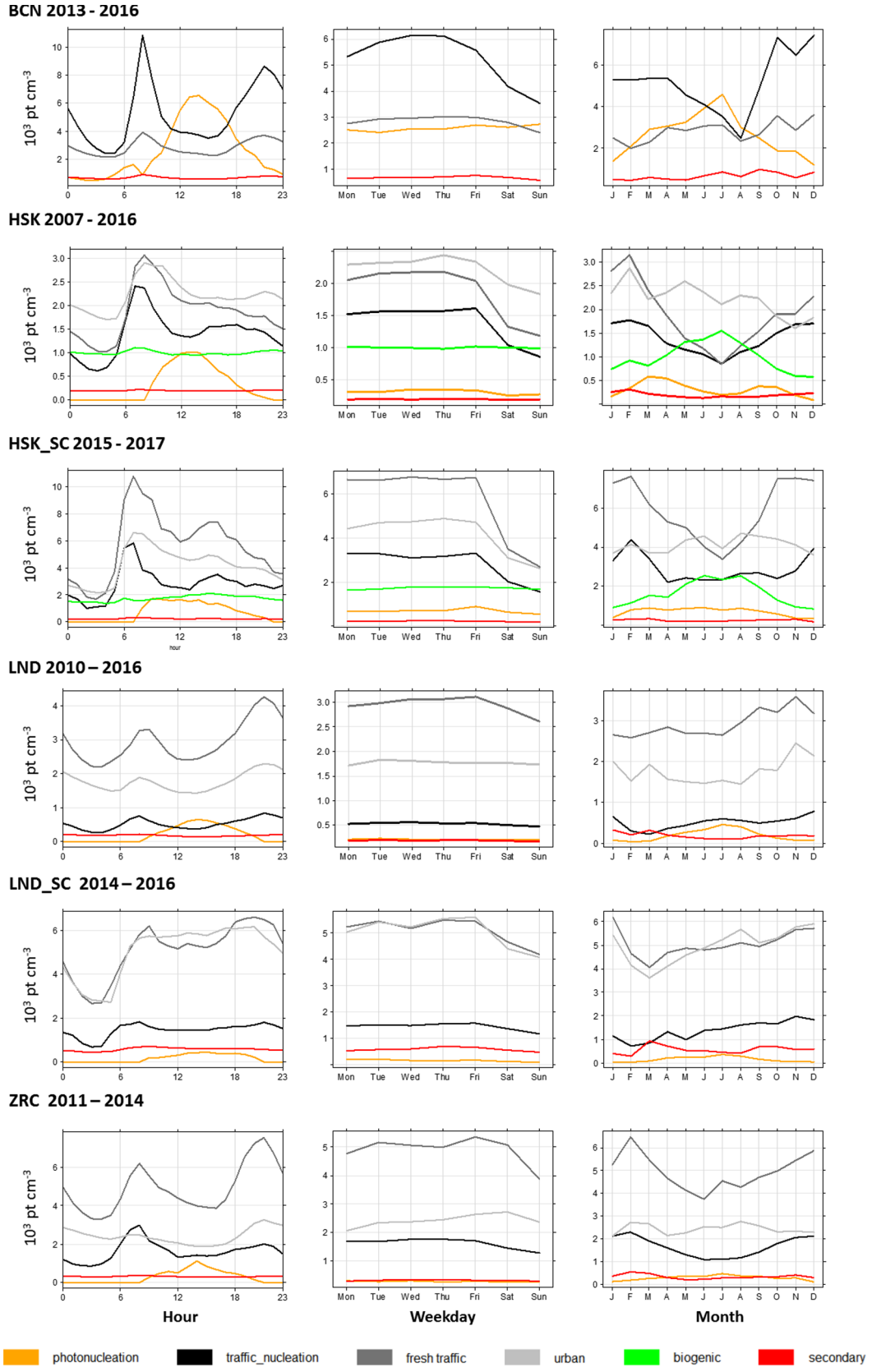

Fig. 3. Daily, weekly and monthly patterns of the sources identified in each city. In Barcelona, *Traffic 1* and *Traffic Nucleation* sources are all included as *Traffic Nucleation*.

Table 5
Average (standard deviation) source contributions at the different sites (only for periods when simultaneous PNSD and NO_x data was available). Total traffic is the addition of *Traffic nucleation*, *Fresh traffic*, and *Urban* (*Traffic (nucleation + fresh)* and *Urban* in the case of BCN).

City		Photo-nucleation (pt cm^{-3})	Traffic nucleation (pt cm^{-3})	Fresh traffic (pt cm^{-3})	Urban (pt cm^{-3})	Total traffic (pt cm^{-3})	Secondary (pt cm^{-3})	Biogenic (pt cm^{-3})
Urban background	BCN PNC_{11-500}	2586 (4310)	5207 (5468)		2835 (2103)	8041 (6973)	675 (573)	–
	HSK PNC_{6-700}	313 (1044)	1391 (1482)	1871 (2546)	2219 (2269)	5481 (4949)	198 (219)	1001 (923)
	LND PNC_{16-600}	203 (619)	527 (625)	2948 (2149)	1770 (1821)	5245 (3480)	184 (269)	–
	ZRC PNC_{10-500}	282 (795)	1621 (1309)	4906 (4626)	2426 (1854)	8952 (6281)	316 (275)	–
Traffic	HSK_SC PNC_{6-800}	694 (2350)	2811 (4050)	5636 (7056)	4156 (3884)	12,603 (12128)	226 (217)	1728 (1447)
	LND_SC PNC_{16-600}	165 (506)	1451 (1242)	5087 (2903)	5037 (3382)	11,575 (6441)	589 (551)	–

Periods of study:
BCN: January 2013 - December 2016; HSK_SC: February 2015 – August 2017; HSK: January 2007 – December 2016; LND_SC: March 2014 – December 2016; LND: January 2010 – December 2016; ZRC: December 2010 - October 2014.

(Niemi et al., 2009). It may also be mixed with secondary aerosols from anthropogenic origin, as we would expect the levels of *Biogenic* source to be lower of what we found during the winter when temperatures are often negative. The influence of anthropogenic secondary aerosols on *Biogenic* is also strengthened by the comparison of the contribution of the sources for the simultaneous periods in HSK and HSK_SC (Table S6), when the *Biogenic* source is higher in HSK_SC than HSK (we would expect similar levels if there were no influence of anthropogenic and traffic emissions). On the other hand, although concentrations of *Secondary* were low all year round, they showed a trend with its minimum during the summer months to some extend explained by the evaporation of ammonium nitrate due to the higher temperatures during summer (Pakkanen et al., 2001). The *Secondary* source may account mainly for anthropogenic emissions, with the total secondary contribution being the addition of the *Secondary* and *Biogenic* sources.

Photonucleation in HSK (annual average = 313 ± 1044 pt cm^{-3}) was higher during the spring (509 ± 1494 pt cm^{-3}) and autumn (310 ± 969 pt cm^{-3}), which coincides with the periods of higher new particle formation in Finland reported in the literature (Dal Maso et al., 2005; Laakso et al., 2003). By looking at the annual pattern of both HSK and HSK_SC (Fig. 3), we suspect that part of the subsequent growth of nucleated particles may be apportioned to the *Urban* source since this source showed maxima in spring and autumn (Laakso et al., 2003). Although the methodologies are not directly comparable, our results are in agreement with the cluster analysis by Hussein et al. (2014) for HSK.

3.5. Sources in London (LND and LND_SC)

Four factors were selected as the solution for PMF in both LND and LND_SC. The sources were identified as *Nucleation* (mode = 21 nm in LND), *Fresh traffic* (37 nm), *Urban* (81 nm), and *Secondary* (294 nm). Although we were expecting a shift towards smaller particles in LND_SC due to proximity to the traffic source, we obtained the same or very similar mode diameters for *Nucleation* (21 nm) and the sources from traffic emissions (34 and 81 nm for *Fresh traffic* and *Urban*, respectively). We obtained a much smaller mode for the *Secondary* aerosols at LND_SC (93 nm; Table 4) but the profile shows a high contribution of particles from around 80 to 300 nm (Fig. 2). The different shape of the profile for the *Secondary* factor in Marylebone may consist of a mix including also traffic non-exhaust emissions as well as cooking, as the latter was identified to be much larger in LND_SC than LND (Ots et al., 2016). PMF was previously applied to PNSD data from 2011 to 2012 from LND (Beddows et al., 2015) and four factors were also identified with very similar profiles to ours.

Fig. 3 shows the diel patterns for *Traffic nucleation*, *Fresh traffic*, and *Urban*. These sources followed the typical pattern of BC and NO_x (common traffic tracers) previously described in literature for LND (North Kensington) and LND_SC (Marylebone; Reche et al., 2011a). In LND, *Urban* was strongly correlated with BC (r = 0.84; Table S5) while *Fresh traffic* showed a moderate correlation (r = 0.53) and *Traffic nucleation* was surprisingly, and unlike what happened at the other sites, not correlated with BC (r = 0.09). For LND_SC, correlation coefficients for BC were stronger (0.52 for *Traffic nucleation*, 0.72 for *Fresh traffic*, and 0.84 for *Urban*) as expected for a street canyon station. Compared to the UB stations in the other cities, LND concentrations of traffic sources were relatively high during the night with a midday local minimum. Moreover, compared to the other cities both LND and LND_SC had stable concentrations of the traffic sources all year round and did not show a minimum over the summer months (Fig. 3). Annual average concentrations (Table 5) were much lower at LND (527 ± 625 pt cm^{-3} for *Traffic Nucleation*, 2948 ± 2149 pt cm^{-3} for *Fresh traffic*, 1770 ± 1821 pt cm^{-3} for *Urban*) than at LND_SC (1451 ± 1242 pt cm^{-3}, 5087 ± 2903 pt cm^{-3}, 5037 ± 2903 pt cm^{-3}, respectively), especially for the source with the smallest particle size which may be associated with fresher emissions (Table S6 shows the annual average for the same periods on both stations). The *Urban* source may also be affected by emissions from biomass burning, which may contribute particularly to the evening peak during the winter months (Fuller et al., 2014; Young et al., 2015). *Urban* showed a higher and maintained evening peak during autumn and winter, which was not present during spring and summer (Fig. S4). In LND, *Photonucleation* was higher during the summer months (398 ± 932 pt cm^{-3}) than the rest of the year (annual average: 203 ± 619 pt cm^{-3}), with very little contribution during the winter (Fig. S4). The same pattern for *Photonucleation* was found at LND_SC but with lower contributions (annual average: 165 ± 506 pt cm^{-3}; summer: 302 ± 723 pt cm^{-3}; winter: 47 ± 195 pt cm^{-3}) as photonucleation processes are usually more important under clean atmospheres (Spracklen et al., 2006). The high PNC in LND_SC may have prevented new particle formation; this point is explored more fully by Bousiotis et al. (2019). Besides the fact that London sites had the largest lower size cut-off, the high PNC in London may also explain the lower *Photonucleation* contribution in comparison with BCN and HSK. Barcelona has considerable pollution levels, however, it experiences very high solar radiation levels and a frequent midday clean up by sea breeze also transporting SO_2 from shipping. On the other hand, Helsinki has lower solar radiation but a much cleaner atmosphere (Table 3). For both London sites, contributions of the *Secondary* aerosol were stable during the day with the minimum found in the early afternoon in LND (Fig. 3), probably associated with the

thermal instability of ammonium nitrate and semi-volatile organic aerosols and with better dispersion conditions of higher wind speeds and mixed layer heights. The annual trend followed the one described for nitrate in London (Revuelta et al., 2012), with lower concentrations during summer (also related to nitrate evaporation) and with higher concentrations from February to April. In LND the weekly pattern of the *Secondary* source showed lower contributions during the weekend (clearly observable when plotting normalised concentrations), which may indicate the influence of local traffic emissions on the secondary particles (also, the correlation with BC reached r = 0.50). Average annual contributions were 184 ± 269 pt cm^{-3} for LND and 589 ± 551 pt cm^{-3} for LND_SC. The coarser nature of the *Secondary* source made it to be the most correlated with PM mass concentrations (r = 0.81 and r = 0.80 for $PM_{2.5}$ in LND and LND_SC, respectively).

3.6. Sources in Zurich (ZRC)

Similar to previous sites, four factors were identified as contributors to PNSD in ZRC. With the exception of the *Secondary* factor, the profiles for ZRC were quite similar to those in LND although the mode diameter for *Nucleation* (15 nm for ZRC) was shifted towards smaller sizes due to smaller lower cut-off of the instrumentation used in ZRC (Fig. 2). The gaseous profile for the *Nucleation* factor was mainly explained by NO_2 and O_3 suggesting the influence of traffic emissions and the presence of photonucleation particles. *Fresh traffic* (33 nm) had a similar mode diameter to BCN while for *Urban* (67 nm) the mode diameter was between the ones found in HSK and BCN (Table 4). The *Secondary* factor showed a bimodal distribution with the main peak in the coarser mode (246 nm).

The average contributions of *Traffic nucleation*, *Fresh traffic*, and *Urban* were 1621 ± 1309 pt cm^{-3}, 4906 ± 4626 pt cm^{-3}, and 2426 ± 1854 pt cm^{-3}, respectively. *Traffic nucleation* and *Fresh traffic* clearly showed the morning traffic peak, while the afternoon peak was followed by *Fresh traffic* and *Urban* (Fig. 3). The diel patterns by season indicate that the relative difference between the morning and afternoon peak was much higher during summer and autumn (Fig. S4). This suggests that both *Fresh traffic* and *Urban*, were possibly affected by other combustion sources, such as solid fuel burning for heating during the cold period or for recreational activities. The daily pattern by day of the week (Fig. S5) allows identification of the drivers of high concentrations in the afternoon peak as these occurred on Friday and Saturday evenings during the warmer months. There is a recreational area with barbequing near the monitoring station. PMF was not able to separate the charcoal or wood combustion used for the barbeques from the traffic sources.

Traffic emissions are the main contributors to *Fresh traffic* and *Traffic nucleation* (and to a lesser extent to *Urban*) since the concentrations diminish considerably during the weekends. The *Secondary* source is very stable over the day (annual average: 316 ± 275 pt cm^{-3}), with a slightly lower concentration in the early afternoon. Similar to other sites, the greatest concentrations of *Secondary* aerosols were observed during the colder months, especially February and March, suggesting that ammonium nitrate may be an important component of the *Secondary* source (since it evaporates during the warmer periods). Minguillón et al. (2012) reported that during wintertime, ammonium nitrate contributed 63.7% of total PM_1 mass concentrations (8.8 μg m^{-3}), which diminished to only 1.5% (0.1 μg m^{-3}) during the summertime. This result suggests that the *Secondary* chemical composition may change over the year since there was not as large a reduction in the PNSD sources. *Photonucleation* contributions showed the expected pattern, with highest levels at midday/early afternoon and during the summer months (summer average: 390 ± 926 pt cm^{-3}; annual average: 316 ± 275 pt cm^{-3}).

3.7. Relative contributions of the sources

Fig. 4 shows the relative contribution of the sources identified by PMF at the different sites. Traffic emissions were by far the highest contributor in all stations, with contributions ranging at maximum (as some traffic sources were mixed with other sources such as biomass burning) from 71 to 91% of the total PNSD. The variability in the absolute average contribution of the combination of traffic sources among the UB sites (ranging from 5245 ± 3480 pt cm^{-3} in LND to 8952 ± 6281 pt cm^{-3} in ZRC; Table 5) partly corresponds to the differences on the lower size cut of the measurement instrument. Generally, the lower the size cut, the greater the number of traffic-emitted particles included in the analysis. This explains the lowest traffic contribution (in absolute terms) in London, where we would expect the contrary (LND has the highest BC and NO_2 concentrations among the UB sites; Table 3). In addition, the relative contribution of the different traffic sources may also be explained by the influence of other sources to these factors as well as the distance to the road of the monitoring site and meteorology, as these variables would affect the amount of time from emission until measurement and the type of physical processes that the particles undergo. For instance, condensation and coagulation implies a growth of the particles (and a number reduction in the case of coagulation), while evaporation is associated with shrinkage (Backman et al., 2012; Yao et al., 2010). The high contribution of traffic emissions to total PNSD has been consistently reported in literature for urban environments around the globe, including the cities in this study (Beddows et al., 2015; Brines et al., 2015; Dall'Osto et al., 2012; Friend et al., 2012; Liu et al., 2014; Pey et al., 2009; Posner and Pandis, 2015; Squizzato et al., 2019; Vu et al., 2015; Wang et al., 2013).

Photonucleation is by far more important in the city with the highest insolation, which is consistent with previous studies (Brines et al., 2015). In BCN, *Photonucleation* represented on average the 23% of the total PNSD, reaching 35% during the period with higher solar radiation (summer) but being significant during the whole year. In the rest of the UB sites, *Photonucleation* contributed on average around 3–4% (Fig. 4), reaching a maximum of 7% in LND (summer) and HSK (spring), and a 5% in ZRC (summer). The contribution of *Photonucleation* in BCN (2586 ± 4310 pt cm^{-3}) was approximately an order of magnitude higher than at the other sites: 313 ± 1044 pt cm^{-3} in HSK, 203 ± 619 pt cm^{-3} in LND, and 282 ± 795 pt cm^{-3} in ZRC. Note that HSK and ZRC lower size cuts (6 and 10 nm, respectively) are lower than in BCN (11 nm) while in LND, the lower size is 16 nm.

Generally, *Secondary* aerosols were the source contributing the least to PNSD (although they would be a large fraction of the mass) due to their regional origin: 3% in LND, HSK, and ZURICH and 6% in BCN. Its relative contribution was generally constant over the year. In HSK, the combination of *Biogenic* and *Secondary* added to a total relative contribution of 17%.

Finally, to provide a consistent comparison, Table S7 shows the annual average of the contributions at the UB stations for the same period at the four cities. The relative contributions for the simultaneous period were very similar to the ones observed for the full period of analysis.

3.8. Spatial origin of ultrafine particles

Fig. 5 shows the polar plots for the different sources and BC, PM_{10}, and SO_2 (if available) in the UB stations, indicating the wind speeds and directions that were associated with higher concentrations of each specific source. The polar plots for the street canyons are presented in Fig. S6.

Traffic sources in BCN were mainly of a local origin since they were predominant at low wind speeds. BCN is influenced by a nearby

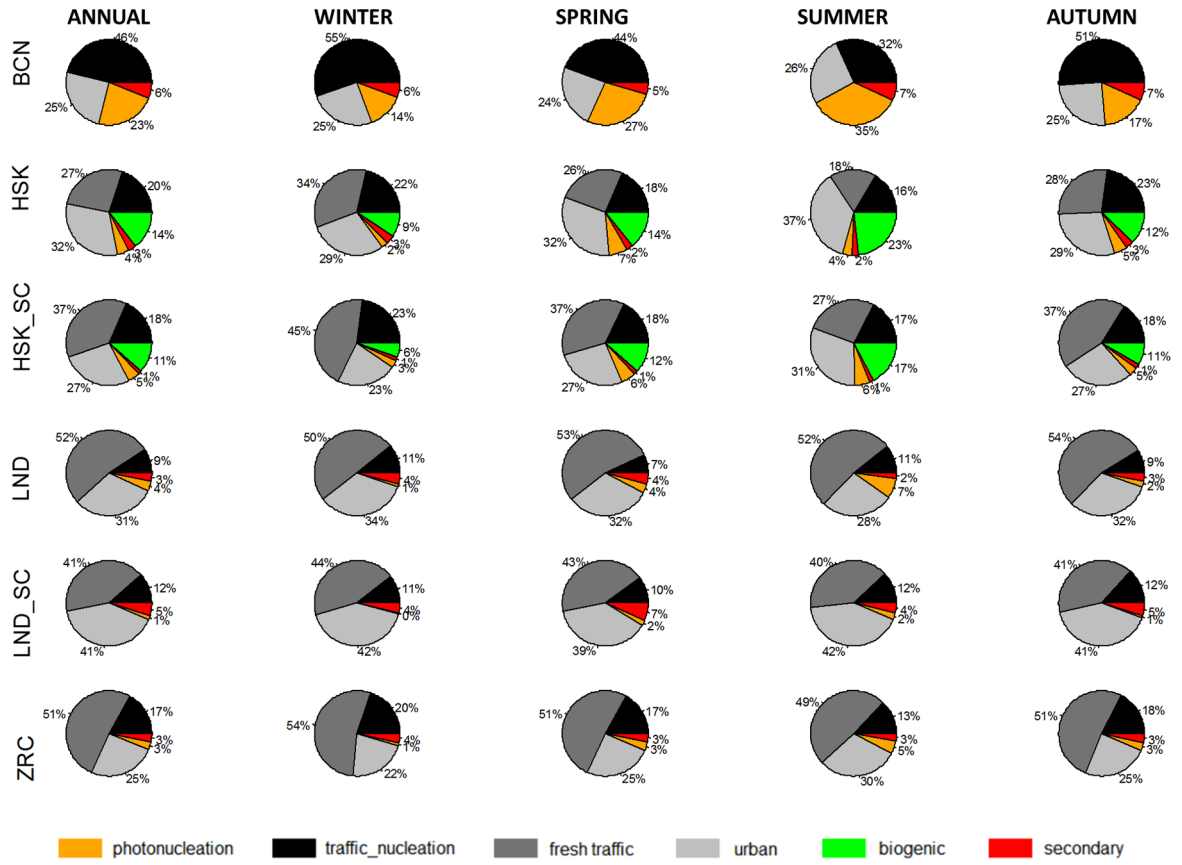

Fig. 4. Relative contribution of the sources at the different station (annual and seasonal averages). In BCN, the source labelled as *Traffic nucleation* corresponds to *Traffic (nucleation + fresh)* (is equivalent to the addition of *Traffic_nucleation* and *Fresh traffic* in the other stations).

important avenue with high traffic intensity. BC followed a similar polar distribution than *Traffic (nucleation + fresh)* and *Urban*. Although *Secondary* particles were also associated with low wind speeds, high contributions of this source were also observed with winds from the E blowing both at low and high wind speeds. The behaviour of *Secondary* particles is broadly mimicking that of PM_{10}, corroborating the secondary and regional origin of the *Secondary* source. SO_2 concentrations were highest for winds blowing from 100 to 180° (especially 160–180°) that is the location of the harbour. Barcelona is registering very low SO_2 levels compared other European cities (Henschel et al., 2013), especially since 2008 when power generation was restricted to only natural gas in the metropolitan area. Thus, currently the main source of SO_2 in the city is shipping. *Photonucleation* particles were associated with light breezes blowing from the S (180–190°). The airport is located about 10 km SSW (185 – 205°) from BCN. Although *Photonucleation* is associated with wind directions that may come from the harbour and airport, we cannot link their emissions with *Photonucleation* due to the low wind speeds and low frequency of winds, especially from the direction of the airport (Fig. S7).

Traffic sources in HSK were associated with N and S wind components (Fig. 5). *Traffic nucleation* was particularly associated with N winds. There are several major roads located N that may have some influence on *Traffic nucleation*, but we would expect a similar or even higher effect (due to particle growth by condensation or coagulation) on *Fresh traffic*, which is not the case. In this direction there is also located the airport, and air traffic is a well know emitter of huge amount of ultrafine particles in the nucleation mode (Hu et al., 2009; Keuken et al., 2015; Masiol and Harrison, 2014; Mazaheri et al., 2009) that can be detected few kilometres away (Cheung et al., 2011; Hudda et al., 2016). The association with high wind speeds may indicate that nucleation particles have to travel fast in order to be detected in such a small size in our receptor station in the UB. Therefore, there might potentially be a contribution from airport emissions to the *Traffic nucleation* source. However, the nucleation mode particles in Helsinki might also originate from several other sources, such as wood combustion in fireplaces and sauna stoves, oil-combustion in boilers, and regional nucleation events. Both *Secondary* and *Biogenic* were associated with winds from the E and, particularly for *Secondary*, covering the angle range to the S - SE.

At HSK_SC the local wind direction results from the orientation of the street canyon relative to the prevailing wind. Thus, prevailing winds are associated with NW and SE (Fig. S7). The *Biogenic* source is associated with N winds (Fig. S6), which, according to the street canyon recirculation dynamics, may actually indicate regional S winds as it did in HSK.

With the exception of *Nucleation* particles (both *Traffic* & *Photonucleation*) in LND, all sources were mainly associated with calm episodes and E winds. This is in agreement with LND being located west of central London and mainland Europe. *Urban* showed a very local contribution (similar to BC) associated with low wind speeds. On the other hand, *Traffic nucleation* and *Photonucleation* were clearly associated with winds blowing from the W – SW sector. Again, although it is difficult to evaluate and quantify, this is pointing towards emission contributions from Heathrow airport (one of the busiest in the world). Moreover, W – SW winds were also associated with clean air masses that favour new particle formation and, therefore, it is difficult to rule out the possible contribution from the airport. Harrison et al. (2019) have also shown an influence of aircraft emissions upon PNSDs at London stations and further analysis of new particle formation events in London is provided by Bousiotis et al. (2019).

At LND_SC, the highest concentrations of traffic sources were observed with E or W winds (same direction as the street canyon) and for

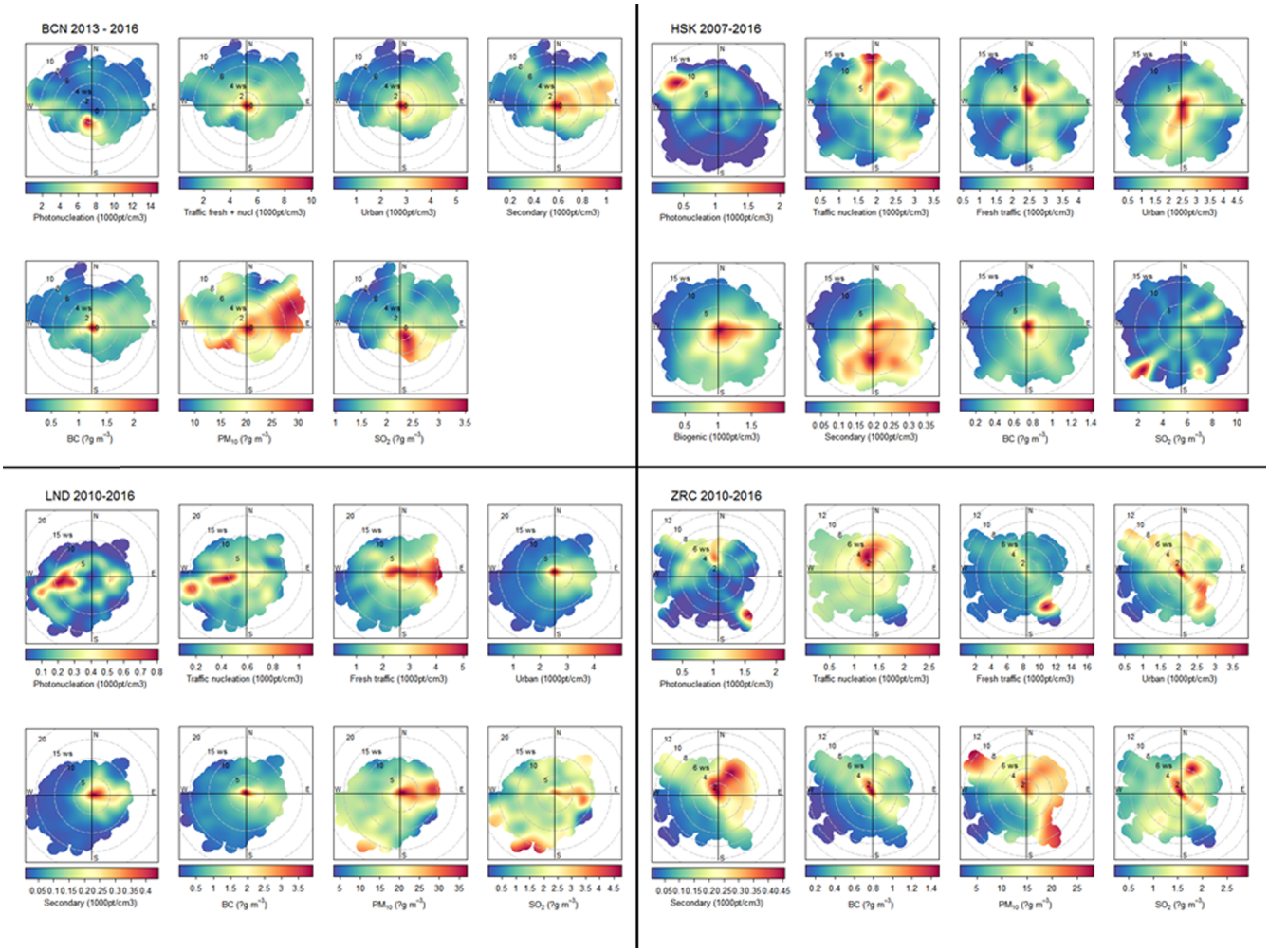

Fig. 5. Polar plots showing how contributions of the different sources and other pollutants were affected by wind direction (angle) and wind speed in (distance from the centre of the plot, m s^{-1}) at the urban background stations.

winds blowing from the S sector. The street canyon recirculation explains the influence of S winds as the station is located in the southern side of the road and, therefore, receives the local pollution of the road when winds blow from the S (Harrison et al., 2019).

In ZRC, *Fresh traffic* and *Urban* sources seem to be mostly associated with SE winds while *Traffic nucleation* was mainly associated with winds from the N sector. *Secondary* particles were mainly associated with local contributions and NE winds. NNE winds are often associated with cold weather forcing the semi-volatile components into the particle phase (particularly ammonium nitrate).

The same results were obtained with the conditional probability function plots (Fig. S8) that indicate the probability of concentrations above the 90th occurring by wind direction and are useful for identify source-areas.

3.9. Influence of airport emissions on urban background stations

The polar plots in Fig. 6 were used to identify possible airport influences on the *Nucleation* particles of the different UB stations. Fig. 6 shows the polar plot for the *Nucleation* factor (before the splitting into *Traffic* and *Photonucleation*) in the first column, the *Traffic nucleation* source in the second, the *Photonucleation* source in the third column, and the *Photonucleation* source for those periods in which there were relatively high *Photonucleation* concentrations even when the environmental conditions were not favourable for the photonucleation process (i.e. low solar radiation – below 80 W m^{-2} – during the winter months). These periods were selected because if photonucleation was low, then airport contributions might be easier to identify. We focused on only the UB stations since the high contribution of traffic emissions in the street canyons might obscure the presence of nucleation particles from the airport.

In Fig. 6, the two dashed lines indicate the angular range of influence of airport emissions: winds blowing from 185 to 205° (SSW) may carry airport emissions to BCN, from 345 to 10° (N) to HSK, from 246 to 260° (WSW) to LND, and 0–22 (NNE) ° to ZRC (the military airport has not been considered due to the low air traffic). In all cases, *Nucleation* particle were observed as being directionally dependent and coincident with the location of city airports. At all the UB stations, *Nucleation* particles were associated with those wind directions that were from the corresponding airport. ZRC has a more complex topography that would induce funnelling and, therefore, the highest concentration were a bit shifted toward NNW instead of NNE. In BCN, the low wind speed may indicate a local origin of the *Nucleation* particles (either *Traffic* or *Photonucleation*) instead of the airport. Alternatively, both HSK and LND showed the coincidence of the airport wind directions with the greatest contributions for *Traffic Nucleation* and *Photonucleation* (under low radiation conditions). However, we note that in HSK there is also several main roads and residential areas with high residential wood combustion emissions at the same direction with the airport. It is difficult to isolate airport emissions contributions without additional tracers; however combining the evidence across the four cities is indicative of airport emissions influencing urban background *Nucleation*

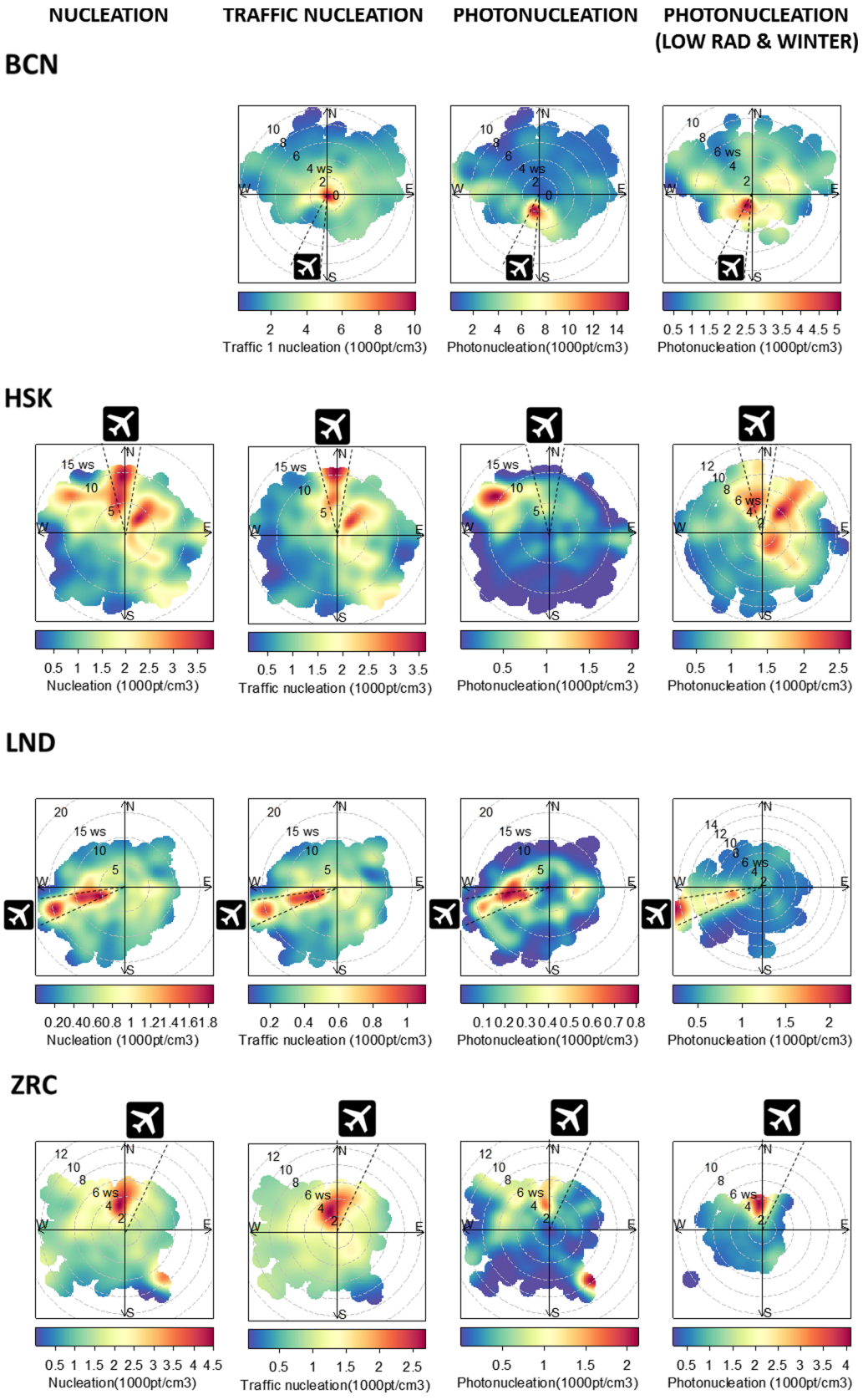

Fig. 6. Polar plots showing how contributions of the Photonucleation source were affected by wind direction and wind speed. The area of influence of the wind direction from the airport is within the dashed lines that convey to the airport sign. Fist column corresponds to the *Nucleation* factor, second column to the *Traffic Nucleation* (or *Traffic (nucleation + fresh)* in the case of BCN), third column corresponds to *Photonucleation* source, and fourth column to the *Photonucleation* source during periods with relatively high *Photonucleation* contribution despite unfavourable conditions for photonucleation processes: low solar radiation (< 80 W m^{-2}) during the coldest and darker months (Nov-Feb). Wind speed units: m s^{-1}.

concentrations. Aircraft emissions are characterised by a PNSD peaking in the nucleation mode (Hu et al., 2009; Keuken et al., 2015; Masiol and Harrison, 2014; Mazaheri et al., 2009). So far, few studies have reported observing an impact of airport emissions in PNSD within urban environments located few kms away (Cheung et al., 2011; Hudda et al., 2016; Keuken et al., 2015).

BC highest concentrations were not associated with wind directions from the airport (Fig. 5) and this may indicate that traffic or wood burning emissions are not the main source of *Nucleation* particles when the wind is blowing from the airport. On the other hand, not identifying high BC concentration from airport direction would be in accordance to aircraft emissions, as aircraft plumes are characterised by very high PNC (especially in the nucleation range) but not BC (Keuken et al., 2015).

Further studies are needed to confirm the potential impact of aircraft emissions and isolate them from other sources.

4. Conclusions

Positive Matrix Factorization (PMF) was used for receptor modelling the source contributions to long time series of hourly size segregated number particle concentrations at six monitoring stations (four urban background and two traffic stations) in four European cities that were affected by different meteorology and emission patterns: Barcelona, Helsinki, London, and Zurich. We identified common sources across all cities: *Photonucleation*, traffic emissions (3 sources, from fresh to aged emissions: *Traffic nucleation*, *Fresh traffic* – mode diameter between 13 and 37 nm-, and *Urban* – mode diameter between 44 and 81 nm), and secondary particles. PMF was able to separate the *Photonucleation* factor only for Barcelona, while a manual split of the *Nucleation* factor (into *Photonucleation* and *Traffic nucleation*) was performed for all the other stations using NO_x concentrations as a proxy for traffic emissions.

Traffic emissions were the main contributor in all stations, with a potential maximum contribution ranging from 71 to 94% of PNSD. For London and Zurich stations, no significant variability among seasons was observed. On the other hand, the high levels of solar radiation in Barcelona led to an important contribution of *Photonucleation* particles (ranging from 14% during the winter period to 35% during summer). Moreover, a source identified as *Biogenic* emissions was only present in Helsinki importantly affecting both the UB and street canyon stations, particularly during summer (23%) but also during spring (14%) and autumn (12%).

When looking at wind directions that were favouring *Nucleation* particles, we observed that in most cases the highest concentrations took place when the wind was blowing from the airport location. Particularly, we could easily identify periods when the urban background station in London was affected by emissions from Heathrow. Although less clear, we found that airport emissions might be as well affecting background PNSD concentrations in Helsinki, Zurich, and Barcelona.

This work provided a detailed characterisation of the sources affecting ultrafine particles in four urban environments in Europe, confirming the great contributions from traffic emissions but also highlighting some differences such as the role of photonucleation in high insolation cities. The contribution of the different sources to PNSD will be used in future studies to evaluate the impact of these specific sources on human health.

CRediT authorship contribution statement

Ioar Rivas: Conceptualization, Methodology, Software, Formal analysis, Writing - original draft, Funding acquisition. **David C.S. Beddows:** Methodology, Software. **Fulvio Amato:** Conceptualization, Methodology, Resources. **David C. Green:** Conceptualization, Methodology. **Leena Järvi:** Investigation, Data curation. **Christoph Hueglin:** Conceptualization, Investigation. **Cristina Reche:** Investigation, Data curation. **Hilkka Timonen:** Investigation, Data curation. **Gary W. Fuller:** Conceptualization, Methodology. **Jarkko Niemi:** Investigation, Data curation. **Noemí Pérez:** Investigation, Data curation. **Minna Aurela:** Investigation, Data curation. **Philip K. Hopke:** Methodology. **Andrés Alastuey:** Conceptualization, Resources. **Markku Kulmala:** Conceptualization, Resources. **Roy M. Harrison:** Conceptualization, Methodology, Supervision. **Xavier Querol:** Conceptualization, Methodology, Supervision, Resources. **Frank J. Kelly:** Conceptualization, Supervision, Funding acquisition.

Declaration of Competing Interest

The authors declare that they have no known competing financial interests or personal relationships that could have appeared to influence the work reported in this paper.

Acknowledgements

This project has received funding from the European Union's Horizon 2020 research and innovation programme under the Marie Skłodowska-Curie grant agreement No 747882. We also thank Academy of Finland Center of Excellence programme (grant no. 307331) and ACTRIS-2 project that receives funding from the European Union Horizon 2020 research and innovation programme under grant agreement No 654109, the "Agencia Estatal de Investigación" from the Spanish Ministry of Science, Innovation and Universities and FEDER funds under the project HOUSE (CGL2016-78594-R).

The authors acknowledge the Departament de Territori i Sostenibilitat and AGAUR (2017 SGR41) from Generalitat de Catalunya, the Faculty of Physics of Barcelona University (Prof. J. Lorente), the Met Office (UK), the Department for Environment, Food and Rural Affairs (DEFRA, UK), and the Swiss Federal Office for the Environment (FOEN) for providing the air pollution and meteorological data.

Appendix A. Supplementary material

Supplementary data to this article can be found online at https://doi.org/10.1016/j.envint.2019.105345.

References

AENA, 2018. Air Traffic Statistics Spain [WWW Document]. URL http://www.aena.es/csee/Satellite?pagename=Estadisticas/Home (accessed 7.12.18).

Amato, F., Alastuey, A., Karanasiou, A., Lucarelli, F., Nava, S., Calzolai, G., Severi, M., Becagli, S., Gianelle, V.L., Colombi, C., Alves, C., Custódio, D., Nunes, T., Cerqueira, M., Pio, C., Eleftheriadis, K., Diapouli, E., Reche, C., Minguillón, M.C., Manousakas, M.I., Maggos, T., Vratolis, S., Harrison, R.M., Querol, X., 2016. AIRUSE-LIFE+: A harmonized PM speciation and source apportionment in five southern European cities. Atmos. Chem. Phys. 16, 3289–3309. https://doi.org/10.5194/acp-16-3289-2016.

Backman, J., Rizzo, L.V., Hakala, J., Nieminen, T., Manninen, H.E., Morais, F., Aalto, P.P., Siivola, E., Carbone, S., Hillamo, R., Artaxo, P., Virkkula, A., Petäjä, T., Kulmala, M., 2012. On the diurnal cycle of urban aerosols, black carbon and the occurrence of new particle formation events in springtime São Paulo, Brazil. Atmos. Chem. Phys. 12, 11733–11751. https://doi.org/10.5194/acp-12-11733-2012.

Beddows, D.C.S., Harrison, R.M., Green, D.C., Fuller, G.W., 2015. Receptor modelling of both particle composition and size distribution from a background site in London, UK. Atmos. Chem. Phys. 15, 10107–10125. https://doi.org/10.5194/acp-15-10107-2015.

BFS, 2016. Mobilität und Verkehr. Neuchâtel, Switzerland.

Bousiotis, D., DallOsto, M., Beddows, D.C.S., Pope, F.D., Harrison, R.M., 2019. Analysis of new particle formation (NPF) events at nearby rural, urban background and urban roadside sites. Atmos. Chem. Phys. 19, 5679–5694. https://doi.org/10.5194/acp-19-5679-2019.

Brewer, E., Li, Y., Finken, B., Quartucy, G., Muzio, L., Baez, A., Garibay, M., Jung, H.S., 2016. PM2.5 and ultrafine particulate matter emissions from natural gas-fired turbine for power generation. Atmos. Environ. 131, 141–149. https://doi.org/10.1016/j.atmosenv.2015.11.048.

Brines, M., Dall'Osto, M., Beddows, D.C.S., Harrison, R.M., Gómez-Moreno, F., Núñez, L., Artíñano, B., Costabile, F., Gobbi, G.P., Salimi, F., Morawska, L., Sioutas, C., Querol, X., 2015. Traffic and nucleation events as main sources of ultrafine particles in high-insolation developed world cities. Atmos. Chem. Phys. 15, 5929–5945. https://doi.

org/10.5194/acp-15-5929-2015.
Carslaw, D.C., Ropkins, K., 2012. Openair - An R package for air quality data analysis. Environ. Model. Softw. 27–28, 52–61. https://doi.org/10.1016/j.envsoft.2011.09.008.
Casati, R., Scheer, V., Vogt, R., Benter, T., 2007. Measurement of nucleation and soot mode particle emission from a diesel passenger car in real world and laboratory in situ dilution. Atmos. Environ. 41, 2125–2135. https://doi.org/10.1016/j.atmosenv.2006.10.078.
Charron, A., Harrison, R.M., 2003. Primary particle formation from vehicle emissions during exhaust dilution in the roadside atmosphere. Atmos. Environ. 37, 4109–4119. https://doi.org/10.1016/S1352-2310(03)00510-7.
Cheung, H.C., Morawska, L., Ristovski, Z.D., 2011. Observation of new particle formation in subtropical urban environment. Atmos. Chem. Phys. 11, 3823–3833. https://doi.org/10.5194/acp-11-3823-2011.
Dal Maso, M., Kulmala, M., Riipinen, I., Wagner, R., Hussein, T., Aalto, P.P., Lehtinen, K.E., 2005. Formation and growth of fresh atmospheric aerosols eight years of aerosol size distribution data from SMEAR. Boreal Environ. Res. 10, 323–336.
Dall'Osto, M., Beddows, D.C.S., Pey, J., Rodriguez, S., Alastuey, A., Harrison, M., Querol, R.X., 2012. Urban aerosol size distributions over the Mediterranean city of Barcelona. NE Spain Atmos. Chem. Phys. 12, 10693–10707. https://doi.org/10.5194/acp-12-10693-2012.
Dall'Osto, M., Querol, X., Alastuey, A., O'Dowd, C., Harrison, R.M., Wenger, J., Gómez-Moreno, F.J., 2013. On the spatial distribution and evolution of ultrafine particles in Barcelona. Atmos. Chem. Phys. 13, 741–759. https://doi.org/10.5194/acp-13-741-2013.
DGT, 2018. Portal estadístico DGT [WWW Document]. URL https://sedeapl.dgt.gob.es/WEB_IEST_CONSULTA/categoria.faces (accessed 7.11.18).
Emami, F., Hopke, P.K., 2017. Effect of adding variables on rotational ambiguity in positive matrix factorization solutions. Chemom. Intell. Lab. Syst. 162, 198–202. https://doi.org/10.1016/j.chemolab.2017.01.012.
Eurostat, 2018. Database - Eurostat [WWW Document]. URL http://ec.europa.eu/eurostat/data/database (accessed 7.11.18).
FINAVIA, 2018. Air Traffic Statistics Finland [WWW Document]. URL https://www.finavia.fi/en/about-finavia/about-air-traffic/traffic-statistics/traffic-statistics-year (accessed 7.12.18).
Friend, A.J., Ayoko, G.A., Jayaratne, E.R., Jamriska, M., Hopke, P.K., Morawska, L., 2012. Source apportionment of ultrafine and fine particle concentrations in Brisbane, Australia. Environ. Sci. Pollut. Res. 19, 2942–2950. https://doi.org/10.1007/s11356-012-0803-6.
Fuller, G.W., Tremper, A.H., Baker, T.D., Yttri, K.E., Butterfield, D., 2014. Contribution of wood burning to PM10in London. Atmos. Environ. 87, 87–94. https://doi.org/10.1016/j.atmosenv.2013.12.037.
Gentner, D.R., Isaacman, G., Worton, D.R., Chan, A.W.H., Dallmann, T.R., Davis, L., Liu, S., Day, D.A., Russell, L.M., Wilson, K.R., Weber, R., Guha, A., Harley, R.A., Goldstein, A.H., 2012. Elucidating secondary organic aerosol from diesel and gasoline vehicles through detailed characterization of organic carbon emissions. Proc. Natl. Acad. Sci. 109, 18318–18323. https://doi.org/10.1073/pnas.1212272109/-/DCSupplemental.www.pnas.org/cgi/doi/10.1073/pnas.1212272109.
Gidhagen, L., Johansson, C., Langner, J., Foltescu, V.L., 2005. Urban scale modeling of particle number concentration in Stockholm. Atmos. Environ. 39, 1711–1725. https://doi.org/10.1016/j.atmosenv.2004.11.042.
Gómez-Moreno, F.J., Alonso, E., Artíñano, B., Juncal-Bello, V., Iglesias-Samitier, S., Iglesias, M.P., Mahía, P.L., Pérez, N., Pey, J., Ripoll, A., Alastuey, A., De La Morena, B.A., García, M.I., Rodríguez, S., Sorribas, M., Titos, G., Lyamani, H., Alados-Arboledas, L., Latorre, E., Tritscher, T., Bischof, O.F., 2015. Intercomparisons of mobility size spectrometers and condensation particle counters in the frame of the Spanish atmospheric observational aerosol network. Aerosol Sci. Technol. 49, 777–785. https://doi.org/10.1080/02786826.2015.1074656.
Gu, J., Pitz, M., Schnelle-Kreis, J., Diemer, J., Reller, A., Zimmermann, R., Soentgen, J., Stoelzel, M., Wichmann, H.E., Peters, A., Cyrys, J., 2011. Source apportionment of ambient particles: Comparison of positive matrix factorization analysis applied to particle size distribution and chemical composition data. Atmos. Environ. 45, 1849–1857. https://doi.org/10.1016/j.atmosenv.2011.01.009.
Harrison, R.M., Beddows, D.C.S., Alam, M.S., Singh, A., Brean, J., Xu, R., Kotthaus, S., Grimmond, S., 2019. Interpretation of particle number size distributions measured across an urban area during the FASTER campaign. Atmos. Chem. Phys. 19, 39–55. https://doi.org/10.5194/acp-19-39-2019.
Harrison, R.M., Rob MacKenzie, A., Xu, H., Alam, M.S., Nikolova, I., Zhong, J., Singh, A., Zeraati-Rezaei, S., Stark, C., Beddows, D.C.S., Liang, Z., Xu, R., Cai, X., 2018. Diesel exhaust nanoparticles and their behaviour in the atmosphere. Proc. R. Soc. A 474. https://doi.org/10.1098/rspa.2018.0492.
Healy, R.M., O'Connor, I.P., Hellebust, S., Allanic, A., Sodeau, J.R., Wenger, J.C., 2009. Characterisation of single particles from in-port ship emissions. Atmos. Environ. 43, 6408–6414. https://doi.org/10.1016/j.atmosenv.2009.07.039.
Helin, A., Niemi, J.V., Virkkula, A., Pirjola, L., Teinilä, K., Backman, J., Aurela, M., Saarikoski, S., Rönkkö, T., Asmi, E., Timonen, H., 2018. Characteristics and source apportionment of black carbon in the Helsinki metropolitan area. Finland. Atmos. Environ. 190, 87–98. https://doi.org/10.1016/j.atmosenv.2018.07.022.
Henschel, S., Querol, X., Atkinson, R., Pandolfi, M., Zeka, A., Le Tertre, A., Analitis, A., Katsouyanni, K., Chanel, O., Pascal, M., Bouland, C., Haluza, D., Medina, S., Goodman, P.G., 2013. Ambient air SO2 patterns in 6 European cities. Atmos. Environ. 79, 236–247. https://doi.org/10.1016/j.atmosenv.2013.06.008.
Hofman, J., Staelens, J., Cordell, R., Stroobants, C., Zikova, N., Hama, S.M.L., Wyche, K.P., Kos, G.P.A., Van Der Zee, S., Smallbone, K.L., Weijers, E.P., Monks, P.S., Roekens, E., 2016. Ultrafine particles in four European urban environments: Results from a new continuous long-term monitoring network. Atmos. Environ. 136, 68–81. https://doi.org/10.1016/j.atmosenv.2016.04.010.
Hu, S., Fruin, S., Kozawa, K., Mara, S., Winer, A.M., Paulson, S.E., 2009. Aircraft emission impacts in a neighborhood adjacent to a general aviation airport in southern California. Environ. Sci. Technol. 43, 8039–8045. https://doi.org/10.1021/es900975f.
Hudda, N., Simon, M.C., Zamore, W., Brugge, D., Durant, J.L., 2016. Aviation emissions impact ambient ultrafine particle concentrations in the greater Boston area. Environ. Sci. Technol. 50, 8514–8521. https://doi.org/10.1021/acs.est.6b01815.
Hussein, T., Mølgaard, B., Hannuniemi, H., Martikainen, J., Järvi, L., Wegner, T., Ripamonti, G., Weber, S., Vesala, T., Hämeri, K., 2014. Fingerprints of the urban particle number size distribution in Helsinki, Finland: Local versus regional characteristics. Boreal Environ. Res. 19, 1–20.
Järvi, L., Hannuniemi, H., Hussein, T., Junninen, H., Aalto, P.P., Hillamo, R., Mäkelä, T., Keronen, P., Siivola, E., Vesala, T., Kulmala, M., 2009. The urban measurement station SMEAR III: Continuous monitoring of air pollution and surface-atmosphere interactions in Helsinki, Finland. Boreal Environ. Res. 14, 86–109. https://doi.org/10.1029/2004JD004936.
Jones, A.M., Harrison, R.M., Barratt, B., Fuller, G., 2012. A large reduction in airborne particle number concentrations at the time of the introduction of " sulphur free" diesel and the London Low Emission Zone. Atmos. Environ. 50, 129–138. https://doi.org/10.1016/j.atmosenv.2011.12.050.
Kasper, A., Aufdenblatten, S., Forss, A., Mohr, M., Burtscher, H., 2007. Particulate emissions from a low-speed marine diesel engine. Aerosol Sci. Technol. 41, 24–32. https://doi.org/10.1080/02786820601055392.
Kasumba, J., Hopke, P.K., Chalupa, D.C., Utell, M.J., 2009. Comparison of sources of submicron particle number concentrations measured at two sites in Rochester, NY. Sci. Total Environ. 407, 5071–5084. https://doi.org/10.1016/j.scitotenv.2009.05.040.
Kettunen, J., Lanki, T., Tiittanen, P., Aalto, P.P., Koskentalo, T., Kulmala, M., Salomaa, V., Pekkanen, J., 2007. Associations of fine and ultrafine particulate air pollution with stroke mortality in an area of low air pollution levels. Stroke 38, 918–922. https://doi.org/10.1161/01.STR.0000257999.49706.3b.
Keuken, M.P., Moerman, M., Zandveld, P., Henzing, J.S., Hoek, G., 2015. Total and size-resolved particle number and black carbon concentrations in urban areas near Schiphol airport (the Netherlands). Atmos. Environ. 104, 132–142. https://doi.org/10.1016/j.atmosenv.2015.01.015.
Kiendler-Scharr, A., Wildt, J., Maso, M.D., Hohaus, T., Kleist, E., Mentel, T.F., Tillmann, R., Uerlings, R., Schurr, U., Wahner, A., 2009. New particle formation in forests inhibited by isoprene emissions. Nature 461, 381–384. https://doi.org/10.1038/nature08292.
Kim, E., Hopke, P.K., Larson, T.V., Covert, D.S., 2004. Analysis of ambient particle size distributions using unmix and positive matrix factorization. Environ. Sci. Technol. 38, 202–209. https://doi.org/10.1021/es030310s.
Kirkby, J., Duplissy, J., Sengupta, K., Frege, C., Gordon, H., Williamson, C., Heinritzi, M., Simon, M., Yan, C., Almeida, J., Trostl, J., Nieminen, T., Ortega, I.K., Wagner, R., Adamov, A., Amorim, A., Bernhammer, A.K., Bianchi, F., Breitenlechner, M., Brilke, S., Chen, X., Craven, J., Dias, A., Ehrhart, S., Flagan, R.C., Franchin, A., Fuchs, C., Guida, R., Hakala, J., Hoyle, C.R., Jokinen, T., Junninen, H., Kangasluoma, J., Kim, J., Krapf, M., Kurten, A., Laaksonen, A., Lehtipalo, K., Makhmutov, V., Mathot, S., Molteni, U., Onnela, A., Perakyla, O., Piel, F., Petaja, T., Praplan, A.P., Pringle, K., Rap, A., Richards, N.A.D., Riipinen, I., Rissanen, M.P., Rondo, L., Sarnela, N., Schobesberger, S., Scott, C.E., Seinfeld, J.H., Sipila, M., Steiner, G., Stozhkov, Y., Stratmann, F., Tomé, A., Virtanen, A., Vogel, A.L., Wagner, A.C., Wagner, P.E., Weingartner, E., Wimmer, D., Winkler, P.M., Ye, P., Zhang, X., Hansel, A., Dommen, J., Donahue, N.M., Worsnop, D.R., Baltensperger, U., Kulmala, M., Carslaw, K.S., Curtius, J., 2016. Ion-induced nucleation of pure biogenic particles. Nature 533, 521–526. https://doi.org/10.1038/nature17953.
Kittelson, D., Watts, W., Johnson, J., 2002. Diesel Aerosol Sampling Methodology - CRC E-43: Final Report, Report for the Coordinating Research Council.
Kittelson, D.B., 1998. Engines and nanoparticles: A review. J. Aerosol Sci. 29, 575–588. https://doi.org/10.1016/S0021-8502(97)10037-4.
Kumar, P., Morawska, L., Birmili, W., Paasonen, P., Hu, M., Kulmala, M., Harrison, R.M., Norford, L., Britter, R., 2014. Ultrafine particles in cities. Environ. Int. 66, 1–10. https://doi.org/10.1016/j.envint.2014.01.013.
Laakso, L., Hussein, T., Aarnio, P., Komppula, M., Hiltunen, V., Viisanen, Y., Kulmala, M., 2003. Diurnal and annual characteristics of particle mass and number concentrations in urban, rural and Arctic environments in Finland. Atmos. Environ. 37, 2629–2641. https://doi.org/10.1016/S1352-2310(03)00206-1.
Lähde, T., Rönkkö, T., Virtanen, A., Schuck, T.J., Pirjola, L., Hämeri, K., Kulmala, M., Arnold, F., Rothe, D., Keskinen, J., 2009. Heavy duty diesel engine exhaust aerosol particle and ion measurements. Environ. Sci. Technol. 43, 163–168. https://doi.org/10.1021/es801690h.
Lanzinger, S., Schneider, A., Breitner, S., Stafoggia, M., Erzen, I., Dostal, M., Pastorkova, A., Bastian, S., Cyrys, J., Zscheppang, A., Kolodnitska, T., Peters, A., 2016. Associations between ultrafine and fine particles and mortality in five central European cities - Results from the UFIREG study. Environ. Int. 88, 44–52. https://doi.org/10.1016/j.envint.2015.12.006.
Leoni, C., Pokorná, P., Hovorka, J., Masiol, M., Topinka, J., Zhao, Y., Křůmal, K., Cliff, S., Mikuška, P., Hopke, P.K., 2018. Source apportionment of aerosol particles at a European air pollution hot spot using particle number size distributions and chemical composition. Environ. Pollut. 234, 145–154. https://doi.org/10.1016/j.envpol.2017.10.097.
Li, X., Yang, K., Han, J., Ying, Q., Hopke, P.K., 2019. Sources of humic-like substances (HULIS) in PM 2.5 in Beijing: Receptor modeling approach. Sci. Total Environ. 671, 765–775. https://doi.org/10.1016/j.scitotenv.2019.03.333.
Liu, Z.R., Hu, B., Liu, Q., Sun, Y., Wang, Y.S., 2014. Source apportionment of urban fine

particle number concentration during summertime in Beijing. Atmos. Environ. 96, 359–369. https://doi.org/10.1016/j.atmosenv.2014.06.055.
Maricq, M.M., Chase, R.E., Xu, N., Laing, P.M., 2002. The effects of the catalytic converter and fuel sulfur level on motor vehicle particulate matter emissions: Light duty diesel vehicles. Environ. Sci. Technol. 36, 283–289. https://doi.org/10.1021/es010962l.
Masiol, M., Harrison, R.M., 2014. Aircraft engine exhaust emissions and other airport-related contributions to ambient air pollution: A review. Atmos. Environ. 95, 409–455. https://doi.org/10.1016/j.atmosenv.2014.05.070.
Mazaheri, M., Johnson, G.R., Morawska, L., 2009. Particle and gaseous emissions from commercial aircraft at each stage of the landing and takeoff cycle. Environ. Sci. Technol. 43, 441–446. https://doi.org/10.1021/es8013985.
McMurry, P.H., Friedlander, S.K., 1979. New particle formation in the presence of an aerosol. Atmos. Environ. 13, 1635–1651. https://doi.org/10.1016/0004-6981(79)90322-6.
Meng, X., Ma, Y., Chen, R., Zhou, Z., Chen, B., Kan, H., 2013. Size-fractionated particle number concentrations and daily mortality in a Chinese City. Environ. Health Perspect. 121, 1174–1178. https://doi.org/10.1289/ehp.1206398.
Meyer, N.K., Ristovski, Z.D., 2007. Ternary nucleation as a mechanism for the production of diesel nanoparticles: Experimental analysis of the volatile and hygroscopic properties of diesel exhaust using the volatilization and humidification tandem differential mobility analyzer. Environ. Sci. Technol. 41, 7309–7314. https://doi.org/10.1021/es062574v.
Minguillón, M.C., Querol, X., Baltensperger, U., Prévôt, A.S.H., 2012. Fine and coarse PM composition and sources in rural and urban sites in Switzerland: local or regional pollution? Sci. Total Environ. 427–428, 191–202. https://doi.org/10.1016/j.scitotenv.2012.04.030.
Morawska, L., Bofinger, N.D., Kocis, L., Nwankwoala, A., 1998. Submicrometer and supermicrometer particles from diesel vehicle emissions. Environ. Sci. Technol. 32, 2033–2042.
Morawska, L., Ristovski, Z., Jayaratne, E.R., Keogh, D.U., Ling, X., 2008. Ambient nano and ultrafine particles from motor vehicle emissions: Characteristics, ambient processing and implications on human exposure. Atmos. Environ. 42, 8113–8138. https://doi.org/10.1016/j.atmosenv.2008.07.050.
Niemi, J.V., Saarikoski, S., Aurela, M., Tervahattu, H., Hillamo, R., Westphal, D.L., Aarnio, P., Koskentalo, T., Makkonen, U., Vehkamäki, H., Kulmala, M., 2009. Long-range transport episodes of fine particles in southern Finland during 1999–2007. Atmos. Environ. 43, 1255–1264. https://doi.org/10.1016/j.atmosenv.2008.11.022.
Ogulei, D., Hopke, P.K., Chalupa, D.C., Utell, M.J., 2007. Modeling source contributions to submicron particle number concentrations measured in Rochester, New York. Aerosol Sci. Technol. 41, 179–201. https://doi.org/10.1080/02786820601116012.
Ogulei, D., Hopke, P.K., Zhou, L., Patrick Pancras, J., Nair, N., Ondov, J.M., 2006. Source apportionment of Baltimore aerosol from combined size distribution and chemical composition data. Atmos. Environ. 40, 396–410. https://doi.org/10.1016/j.atmosenv.2005.11.075.
Ohlwein, S., Kappeler, R., Kutlar Joss, M., Künzli, N., Hoffmann, B., 2019. Health effects of ultrafine particles: a systematic literature review update of epidemiological evidence. Int. J. Public Health 7. https://doi.org/10.1007/s00038-019-01202-7.
Ots, R., Vieno, M., Allan, J.D., Reis, S., Nemitz, E., Young, D.E., Coe, H., Di Marco, C., Detournay, A., Mackenzie, I.A., Green, D.C., Heal, M.R., 2016. Model simulations of cooking organic aerosol (COA) over the UK using estimates of emissions based on measurements at two sites in London. Atmos. Chem. Phys. 16, 13773–13789. https://doi.org/10.5194/acp-16-13773-2016.
Paatero, P., 1999. The multilinear engine—a table-driven, least squares program for solving multilinear problems, including the n-way parallel factor analysis model. J. Comput. Graph. Stat. 8, 854–888. https://doi.org/10.1080/10618600.1999.10474853.
Paatero, P., 1997. Least squares formulation of robust non-negative factor analysis. Chemom. Intell. Lab. Syst. 37, 23–35. https://doi.org/10.1016/S0169-7439(96)00044-5.
Pakkanen, T.A., Kerminen, V.M., Korhonen, C.H., Hillamo, R.E., Aarnio, P., Koskentalo, T., Maenhaut, W., 2001. Urban and rural ultrafine (PM0.1) particles in the Helsinki area. Atmos. Environ. 35, 4593–4607. https://doi.org/10.1016/S1352-2310(01)00167-4.
Pancras, J.P., Landis, M.S., Norris, G.A., Vedantham, R., Dvonch, J.T., 2013. Source apportionment of ambient fine particulate matter in Dearborn, Michigan, using hourly resolved PM chemical composition data. Sci. Total Environ. https://doi.org/10.1016/j.scitotenv.2012.11.083.
Pandolfi, M., Alastuey, A., Pérez, N., Reche, C., Castro, I., Shatalov, V., Querol, X., 2016. Trends analysis of PM source contributions and chemical tracers in NE Spain during 2004–2014: A multi-exponential approach. Atmos. Chem. Phys. 16, 11787–11805. https://doi.org/10.5194/acp-16-11787-2016.
Park, S.S., Kozawa, K., Fruin, S., Mara, S., Hsu, Y.-K., Jakober, C., Winer, A., Herner, J., 2017. Emission factors for high-emitting vehicles based on on-road measurements of individual vehicle exhaust with a mobile measurement platform. J. Air Waste Manage. Assoc. 61, 1046–1056. https://doi.org/10.1080/10473289.2011.595981.
Pey, J., Querol, X., Alastuey, A., Rodríguez, S., Putaud, J.P., Van Dingenen, R., 2009. Source apportionment of urban fine and ultra-fine particle number concentration in a Western Mediterranean city. Atmos. Environ. 43, 4407–4415. https://doi.org/10.1016/j.atmosenv.2009.05.024.
Pey, J., Rodríguez, S., Querol, X., Alastuey, A., Moreno, T., Putaud, J.P., Van Dingenen, R., 2008. Variations of urban aerosols in the western Mediterranean. Atmos. Environ. 42, 9052–9062. https://doi.org/10.1016/j.atmosenv.2008.09.049.
Port of Helsinki, 2018. Port of Helsinki Annual Report 2017 [WWW Document]. URL https://www.portofhelsinki.fi/en/port-helsinki/publications-and-statistics (accessed 7.12.18).
Posner, L.N., Pandis, S.N., 2015. Sources of ultrafine particles in the Eastern United States. Atmos. Environ. 111, 103–112. https://doi.org/10.1016/j.atmosenv.2015.03.033.
R Core Team, 2018. R: A language and environment for statistical computing.
Rantala, P., Järvi, L., Taipale, R., Laurila, T.K., Patokoski, J., Kajos, M.K., Kurppa, M., Haapanala, S., Siivola, E., Petäjä, T., Ruuskanen, T.M., Rinne, J., 2016. Anthropogenic and biogenic influence on VOC fluxes at an urban background site in Helsinki, Finland. Atmos. Chem. Phys. 16, 7981–8007. https://doi.org/10.5194/acp-16-7981-2016.
Reche, C., Querol, X., Alastuey, A., Viana, M., Pey, J., Moreno, T., Rodríguez, S., González, Y., Fernández-Camacho, R., de la Rosa, J., Dall'Osto, M., Prévôt, A.S.H., Hueglin, C., Harrison, R.M., Quincey, P., 2011a. New considerations for PM, Black Carbon and particle number concentration for air quality monitoring across different European cities. Atmos. Chem. Phys. 11, 6207–6227. https://doi.org/10.5194/acp-11-6207-2011.
Reche, C., Viana, M., Moreno, T., Querol, X., Alastuey, A., Pey, J., Pandolfi, M., Prévôt, A., Mohr, C., Richard, A., Artiñano, B., Gomez-Moreno, F.J., Cots, N., 2011b. Peculiarities in atmospheric particle number and size-resolved speciation in an urban area in the western Mediterranean: Results from the DAURE campaign. Atmos. Environ. 45, 5282–5293. https://doi.org/10.1016/j.atmosenv.2011.06.059.
Revuelta, M.A., Harrison, R.M., Núñez, L., Gomez-Moreno, F.J., Pujadas, M., Artíñano, B., 2012. Comparison of temporal features of sulphate and nitrate at urban and rural sites in Spain and the UK. Atmos. Environ. 60, 383–391. https://doi.org/10.1016/j.atmosenv.2012.07.004.
Ripamonti, G., Järvi, L., Mølgaard, B., Hussein, T., Nordbo, A., Hämeri, K., 2013. The effect of local sources on aerosol particle number size distribution, concentrations and fluxes in Helsinki, Finland. Tellus, Ser. B Chem. Phys. Meteorol. 65. https://doi.org/10.3402/tellusb.v65i0.19786.
Robinson, A.L., Donahue, N.M., Shrivastava, M.K., Weitkamp, E.A, Sage, A.M., Grieshop, A.P., Lane, T.E., Pierce, J.R., Pandis, S.N., 2007. Rethinking organic aerosols: semi-volatile emissions and photochemical aging. Science (80). 315, 1259–1262. 10.1126/science.1133061.
Rodríguez, S., Cuevas, E., 2007. The contributions of "minimum primary emissions" and "new particle formation enhancements" to the particle number concentration in urban air. J. Aerosol Sci. 38, 1207–1219. https://doi.org/10.1016/j.jaerosci.2007.09.001.
Rönkkö, T., Kuuluvainen, H., Karjalainen, P., Keskinen, J., Hillamo, R., Niemi, J.V., Pirjola, L., Timonen, H.J., Saarikoski, S., Saukko, E., Järvinen, A., Silvennoinen, H., Rostedt, A., Olin, M., Yli-Ojanperä, J., Nousiainen, P., Kousa, A., Dal Maso, M., 2017. Traffic is a major source of atmospheric nanocluster aerosol. Proc. Natl. Acad. Sci. 114, 7549–7554. https://doi.org/10.1073/pnas.1700830114.
Rönkkö, T., Lähde, T., Heikkilä, J., Pirjola, L., Bauschke, U., Arnold, F., Schlager, H., Rothe, D., Yli-Ojanperä, J., Keskinen, J., 2013. Effects of gaseous sulphuric acid on diesel exhaust nanoparticle formation and characteristics. Environ. Sci. Technol. 47, 11882–11889. https://doi.org/10.1021/es402354y.
Rönkkö, T., Pirjola, L., Ntziachristos, L., Heikkilä, J., Karjalainen, P., Hillamo, R., Keskinen, J., 2014. Vehicle engines produce exhaust nanoparticles even when not fueled. Environ. Sci. Technol. 48, 2043–2050. https://doi.org/10.1021/es405687m.
Rönkkö, T., Virtanen, A., Vaaraslahti, K., Keskinen, J., Pirjola, L., Lappi, M., 2006. Effect of dilution conditions and driving parameters on nucleation mode particles in diesel exhaust: Laboratory and on-road study. Atmos. Environ. 40, 2893–2901. https://doi.org/10.1016/j.atmosenv.2006.01.002.
Samoli, E., Andersen, Z.J., Katsouyanni, K., Hennig, F., Kuhlbusch, T.A.J., Bellander, T., Cattani, G., Cyrys, J., Forastiere, F., Jacquemin, B., Kulmala, M., Lanki, T., Loft, S., Massling, A., Tobias, A., Stafoggia, M., 2016. Exposure to ultrafine particles and respiratory hospitalisations in five European cities. Eur. Respir. J. 48, 674–682. https://doi.org/10.1183/13993003.02108-2015.
Sgro, L.A., Borghese, A., Speranza, L., Barone, A.C., Minutolo, P., Bruno, A., D'Anna, A., D'Alessio, A., 2008. Measurements of nanoparticles of organic carbon and soot in flames and vehicle exhausts. Environ. Sci. Technol. 42, 859–863. https://doi.org/10.1021/es070485s.
Shi, J.P., Evans, D.E., Khan, A.A., Harrison, R.M., 2001. Sources and concentration of nanoparticles (< 10 nm diameter) in the urban atmosphere. Atmos. Environ. 35, 1193–1202.
Shi, J.P., Harrison, R.M., 1999. Investigation of ultrafine particle formation during diesel exhaust dilution. Environ. Sci. Technol. 33, 3730–3736. https://doi.org/10.1021/es9811871.
Sioutas, C., Delfino, R.J., Singh, M., 2005. Exposure assessment for atmospheric ultrafine particles (UFPs) and implications in epidemiologic research. Environ. Health Perspect. 113, 947–955. https://doi.org/10.1289/ehp.7939.
Sowlat, M.H., Hasheminassab, S., Sioutas, C., 2016. Source apportionment of ambient particle number concentrations in central Los Angeles using positive matrix factorization (PMF). Atmos. Chem. Phys. 16, 4849–4866. https://doi.org/10.5194/acp-16-4849-2016.
Spracklen, D.V., Carslaw, K.S., Kulmala, M., Kerminen, V.M., Mann, G.W., Sihto, S.L., 2006. The contribution of boundary layer nucleation events to total particle concentrations on regional and global scales. Atmos. Chem. Phys. 6, 5631–5648. https://doi.org/10.5194/acp-6-5631-2006.
Squizzato, S., Masiol, M., Emami, F., Chalupa, D.C., Utell, M.J., Rich, D.Q., Hopke, P.K., 2019. Long-term changes of source apportioned particle number concentrations in a metropolitan area of the northeastern United States. Atmosphere (Basel) 10. https://doi.org/10.3390/atmos10010027.
Stafoggia, M., Schneider, A., Cyrys, J., Samoli, E., Andersen, Z.J., Bedada, G.B., Bellander, T., Cattani, G., Eleftheriadis, K., Faustini, A., Hoffmann, B., Jacquemin, B., Katsouyanni, K., Massling, A., Pekkanen, J., Perez, N., Peters, A., Quass, U., Yli-Tuomi, T., Forastiere, F., 2017. Association between short-term exposure to ultrafine particles and mortality in eight European Urban Areas. Epidemiology 28, 172–180.

https://doi.org/10.1097/EDE.0000000000000599.
Statistics Finland, 2018. Web databases [WWW Document]. URL http://pxnet2.stat.fi/PXWeb/pxweb/en/StatFin/StatFin_lii_mkan/statfin_mkan_pxt_002.px/?rxid=e896c495-8a24-4d09-a221-2bb2ad507456 (accessed 7.11.18).
Sun, J., Birmili, W., Hermann, M., Tuch, T., Weinhold, K., Spindler, G., Schladitz, A., Bastian, S., Löschau, G., Cyrys, J., Gu, J., Flentje, H., Briel, B., Asbach, C., Kaminski, H., Ries, L., Sohmer, R., Gerwig, H., Wirtz, K., Meinhardt, F., Schwerin, A., Bath, O., Ma, N., Wiedensohler, A., 2019. Variability of black carbon mass concentrations, submicrometer particle number concentrations and size distributions: results of the German Ultrafine Aerosol Network ranging from city street to High Alpine locations. Atmos. Environ. 202, 256–268. https://doi.org/10.1016/j.atmosenv.2018.12.029.
Tobías, A., Rivas, I., Reche, C., Alastuey, A., Rodríguez, S., Fernández-Camacho, R., Sánchez de la Campa, A.M., de la Rosa, J., Sunyer, J., Querol, X., 2018. Short-term effects of ultrafine particles on daily mortality by primary vehicle exhaust versus secondary origin in three Spanish cities. Environ. Int. 111, 144–151. https://doi.org/10.1016/j.envint.2017.11.015.
Tobias, H.J., Beving, D.E., Ziemann, P.J., Sakurai, H., Zuk, M., McMurry, P.H., Zarling, D., Waytulonis, R., Kittelson, D.B., 2001. Chemical analysis of diesel engine nanoparticles using a nano-DMA/thermal desorption particle beam mass spectrometer. Environ. Sci. Technol. 35, 2233–2243. https://doi.org/10.1021/es0016654.
UK Met Office, 2006. MIDAS: Global Radiation Observations [WWW Document]. NCAS Br. Atmos. Data Cent. URL http://catalogue.ceda.ac.uk/uuid/b4c028814a666a651f52f2b37a97c7c7 (accessed 4.23.18).
UK NAEI, 2014. National Atmospheric Emisisons Inventory: Base 2013 fleet composition projections data.
Van Buuren, S., Groothuis-Oudshoorn, K., 2011. Multivariate imputation by chained equations. J. Stat. Softw. 45, 1–67. https://doi.org/10.1177/0962280206074463.
Viana, M., Kuhlbusch, T.A.J., Querol, X., Alastuey, A., Harrison, R.M., Hopke, P.K., Winiwarter, W., Vallius, M., Szidat, S., Prévôt, A.S.H., Hueglin, C., Bloemen, H., Wåhlin, P., Vecchi, R., Miranda, A.I., Kasper-Giebl, A., Maenhaut, W., Hitzenberger, R., 2008. Source apportionment of particulate matter in Europe: A review of methods and results. J. Aerosol Sci. 39, 827–849. https://doi.org/10.1016/j.jaerosci.2008.05.007.
Volkamer, R., Jimenez, J.L., San Martini, F., Dzepina, K., Zhang, Q., Salcedo, D., Molina, L.T., Worsnop, D.R., Molina, M.J., 2006. Secondary organic aerosol formation from anthropogenic air pollution: Rapid and higher than expected. Geophys. Res. Lett. 33, 7–10. https://doi.org/10.1029/2006GL026899.
Von Bismarck-Osten, C., Birmili, W., Ketzel, M., Massling, A., Petäjä, T., Weber, S., 2013. Characterization of parameters influencing the spatio-temporal variability of urban particle number size distributions in four European cities. Atmos. Environ. 77, 415–429. https://doi.org/10.1016/j.atmosenv.2013.05.029.
Vu, T.V., Delgado-Saborit, J.M., Harrison, R.M., 2015. Review: Particle number size distributions from seven major sources and implications for source apportionment studies. Atmos. Environ. 122, 114–132. https://doi.org/10.1016/j.atmosenv.2015.09.027.
Wang, F., Ketzel, M., Ellermann, T., Wåhlin, P., Jensen, S.S., Fang, D., Massling, A., 2010. Particle number, particle mass and NOx emission factors at a highway and an urban street in Copenhagen. Atmos. Chem. Phys. 10, 2745–2764. https://doi.org/10.5194/acp-10-2745-2010.
Wang, H., Shooter, D., 2005. Source apportionment of fine and coarse atmospheric particles in Auckland, New Zealand. Sci. Total Environ. 340, 189–198. https://doi.org/10.1016/j.scitotenv.2004.08.017.
Wang, Y., Hopke, P.K., Chalupa, D.C., Utell, M.J., 2011a. Effect of the shutdown of a coal-fired power plant on urban ultrafine particles and other pollutants. Aerosol Sci. Technol. 45, 1245–1249. https://doi.org/10.1080/02786826.2011.588730.
Wang, Y., Hopke, P.K., Chalupa, D.C., Utell, M.J., 2011b. Long-term study of urban ultrafine particles and other pollutants. Atmos. Environ. 45, 7672–7680. https://doi.org/10.1016/j.atmosenv.2010.08.022.
Wang, Z.B., Hu, M., Wu, Z.J., Yue, D.L., He, L.Y., Huang, X.F., Liu, X.G., Wiedensohler, A., 2013. Long-term measurements of particle number size distributions and the relationships with air mass history and source apportionment in the summer of Beijing. Atmos. Chem. Phys. 13, 10159–10170. https://doi.org/10.5194/acp-13-10159-2013.
WHO, 2018. Global urban ambient air pollution database.
Wiedensohler, A., Birmili, W., Nowak, A., Sonntag, A., Weinhold, K., Merkel, M., Wehner, B., Tuch, T., Pfeifer, S., Fiebig, M., Fjäraa, A.M., Asmi, E., Sellegri, K., Depuy, R., Venzac, H., Villani, P., Laj, P., Aalto, P., Ogren, J.A., Swietlicki, E., Williams, P., Roldin, P., Quincey, P., Hüglin, C., Fierz-Schmidhauser, R., Gysel, M., Weingartner, E., Riccobono, F., Santos, S., Grüning, C., Faloon, K., Beddows, D., Harrison, R., Monahan, C., Jennings, S.G., O'Dowd, C.D., Marinoni, A., Horn, H.G., Keck, L., Jiang, J., Scheckman, J., McMurry, P.H., Deng, Z., Zhao, C.S., Moerman, M., Henzing, B., De Leeuw, G., Löschau, G., Bastian, S., 2012. Mobility particle size spectrometers: Harmonization of technical standards and data structure to facilitate high quality long-term observations of atmospheric particle number size distributions. Atmos. Meas. Tech. 5, 657–685. https://doi.org/10.5194/amt-5-657-2012.
Wiedensohler, A., Wiesner, A., Weinhold, K., Birmili, W., Hermann, M., Merkel, M., Müller, T., Pfeifer, S., Schmidt, A., Tuch, T., Velarde, F., Quincey, P., Seeger, S., Nowak, A., 2018. Mobility particle size spectrometers: Calibration procedures and measurement uncertainties. Aerosol Sci. Technol. 52, 146–164. https://doi.org/10.1080/02786826.2017.1387229.
Yan, C., Dada, L., Rose, C., Jokinen, T., Nie, W., Schobesberger, S., Junninen, H., Lehtipalo, K., Sarnela, N., Makkonen, U., Garmash, O., Wang, Y., Zha, Q., Paasonen, P., Bianchi, F., Sipilä, M., Ehn, M., Petäjä, T., Kerminen, V.-M., Worsnop, D.R., Kulmala, M., 2018. The role of H2SO4-NH3 anion clusters in ion-induced aerosol nucleation mechanisms in the boreal forest. Atmos. Chem. Phys. Discuss. 18, 13231–13243. https://doi.org/10.5194/acp-2018-187.
Yao, X., Choi, M.Y., Lau, N.T., Lau, A.P.S., Chan, C.K., Fang, M., 2010. Growth and shrinkage of new particles in the atmosphere in Hong Kong. Aerosol Sci. Technol. 44, 639–650. https://doi.org/10.1080/02786826.2010.482576.
Yao, X., Lau, N.T., Fang, M., Chan, C.K., 2005. Real-time observation of the transformation of ultrafine atmospheric particle modes. Aerosol Sci. Technol. 39, 831–841. https://doi.org/10.1080/02786820500295248.
Young, D.E., Allan, J.D., Williams, P.I., Green, D.C., Flynn, M.J., Harrison, R.M., Yin, J., Gallagher, M.W., Coe, H., 2015. Investigating the annual behaviour of submicron secondary inorganic and organic aerosols in London. Atmos. Chem. Phys. 15, 6351–6366. https://doi.org/10.5194/acp-15-6351-2015.
Yu, X., Venecek, M., Hu, J., Tanrikulu, S., Soon, S.-T., Tran, C., Fairley, D., Kleeman, M.J., 2018. Sources of airborne ultrafine particle number and mass concentrations in California. Atmos. Chem. Phys. Discuss. 1–37. https://doi.org/10.5194/acp-2018-832.
Yue, W., Stölzel, M., Cyrys, J., Pitz, M., Heinrich, J., Kreyling, W.G., Wichmann, H.E., Peters, A., Wang, S., Hopke, P.K., 2008. Source apportionment of ambient fine particle size distribution using positive matrix factorization in Erfurt, Germany. Sci. Total Environ. 398, 133–144. https://doi.org/10.1016/j.scitotenv.2008.02.049.
Zhou, L., Kim, E., Hopke, P.K., Stanier, C., Pandis, S.N., 2005. Mining airborne particulate size distribution data by positive matrix factorization. J. Geophys. Res. Atmos. 110, 1–15. https://doi.org/10.1029/2004JD004707.
Zhou, L., Kim, E., Hopke, P.K., Stanier, C.O., Pandis, S., 2004. Advanced factor analysis on Pittsburgh particle size-distribution data. Aerosol Sci. Technol. 38, 118–132. https://doi.org/10.1080/02786820390229589.
Zhu, Y., Hinds, W.C., Kim, S., Shen, S., Sioutas, C., 2002. Study of ultrafine particles near a major highway with heavy-duty diesel traffic. Atmos. Environ. 36, 4323–4335. https://doi.org/10.1016/S1352-2310(02)00354-0.